

3-D FINITE ELEMENT ANALYSIS OF SEMI-RIGID  
STEEL CONNECTIONS

A THESIS SUBMITTED TO  
THE GRADUATE SCHOOL OF NATURAL AND APPLIED SCIENCES  
OF  
MIDDLE EAST TECHNICAL UNIVERSITY

BY

CAFER HARUN USLU

IN PARTIAL FULFILLMENT OF THE REQUIREMENTS  
FOR  
THE DEGREE OF MASTER OF SCIENCE  
IN  
CIVIL ENGINEERING

JULY 2009

Approval of the thesis:

**3-D FINITE ELEMENT ANALYSIS OF SEMI-RIGID  
STEEL CONNECTIONS**

submitted by **CAFER HARUN USLU** in partial fulfillment of the requirements for  
the degree of **Master of Science in Civil Engineering Department, Middle East  
Technical University** by,

Prof. Dr. Canan Özgen  
Dean, Graduate School of **Natural and Applied Sciences**

\_\_\_\_\_

Prof. Dr. Güney Özcebe  
Head of Department, **Civil Engineering**

\_\_\_\_\_

Asst. Prof. Dr. Afşin Sarıtaş  
Supervisor, **Civil Engineering Dept., METU**

\_\_\_\_\_

**Examining Committee Members**

Assoc. Prof. Dr. Cem Topkaya  
Civil Engineering Dept., METU

\_\_\_\_\_

Asst. Prof. Afşin Sarıtaş  
Civil Engineering Dept., METU

\_\_\_\_\_

Asst. Prof. Dr. Alp Caner  
Civil Engineering Dept., METU

\_\_\_\_\_

Asst. Prof. Dr. Yalın Arıcı  
Civil Engineering Dept., METU

\_\_\_\_\_

Asst. Prof. Dr. Eray Baran  
Civil Engineering Dept., Atılım University

\_\_\_\_\_

**Date:** 28.07.2009

**I hereby declare that all information in this document has been obtained and presented in accordance with academic rules and ethical conduct. I also declare that, as required by these rules and conduct, I have fully cited and referenced all material and results that are not original to this work.**

Name, Last name: **Cafer Harun USLU**

Signature :

## **ABSTRACT**

### **3-D FINITE ELEMENT ANALYSIS OF SEMI-RIGID STEEL CONNECTIONS**

Uslu, Cafer Harun

M.S., Department of Civil Engineering

Supervisor: Asst. Prof. Dr. Afşin Sarıtaş

July 2009, 75 Pages

Two types of connection are generally considered in the design of steel structures in practice. These are classified as completely rigid (moment) and simple (shear) connections. In theory, completely rigid connections can not undergo rotation and simple connections can not transfer moment. However, in reality rigid connections have a relative flexibility which makes them to rotate and simple connections have some reserve capacity to transfer moments. In many modern design specifications, this fact is realized and another type which is called partially restrained or semi-rigid connection is introduced. These types of connections have got the transfer of some beam moment to column together with shear. However, there is a lack of information on the amount of moment transferred and rotation of connection during the action of the moment transfer. The only way to quantify the moment and rotation of the partially restrained connections is to draw moment-rotation curves. Nevertheless, drawing such curves requires great amount of expenses for experiments. Taking these into account, the use of finite elements with the help of increased computational power is one way to obtain moment-rotation curves of connections.

Available test results guides the finite element analysis for justifications. So these analyses can be further implemented into design functions. This thesis is intended to conduct 3-D non-linear finite element analyses to compliment with tests results for different types of semi-rigid connections with angles and compare them with mathematical models developed by different researchers.

Keywords: Semi-Rigid Beam to Column Steel Connections, 3-D Nonlinear Finite Element Analysis, Mathematical Models for Semi-Rigid Connections

## ÖZ

### YARI RİJİT ÇELİK BAĞLANTILARIN 3-D SONLU ELEMANLAR İLE ANALİZİ

Uslu, Cafer Harun

Yüksek Lisans, İnşaat Mühendisliği Bölümü

Tez Yöneticisi: Yard.Doç.Dr. Afşin Sarıtaş

Temmuz 2009, 75 Sayfa

Pratikte, tasarım gereksinimleri için genellikle iki tip bağlantı göz önüne alınmaktadır. Bunlar tamamen rijit (moment) ve basit (mafsal) bağlantılardır. Teoride tamamen rijit bağlantılar herhangi bir dönme hareketi yapamazlar ve basit bağlantılarsa moment taşıyamazlar. Gerçek durumdaysa, rijit bağlantılar kendilerini dönebilir kılan bir miktar esnekliğe ve basit bağlantılar bir miktar rezerve moment kapasitesine sahiptirler. Günümüzdeki birçok modern tasarım standardı bu gerçeği fark ederek yarı rijit adı verilen bir bağlantı türünü gündeme getirmiştir. Bu bağlantı tipi kiriş momentinin bir kısmını kesme kuvveti ile birlikte kolona taşıyabilecek kapasiteye sahiptir. Fakat aktarılan moment miktarı ve buna bağlı dönme hareketinin miktarı konusunda bilgi eksikliği bulunmaktadır. Kısmi bağlı bağlantıların moment ve dönme değerlerinin bulunabilmesinin tek yolu moment-dönme eğrilerinin çizilmesidir. Bu arada bu eğrilerin çizilmesi için gereken testler büyük miktarda maliyete gereksinim duymaktadır. Bunlar göz önüne alındığında, bu tip bağlantıların dijital bilgisayarlar kullanılarak sonlu elemanlar analiziyle modellenmeye çalışılması, moment-dönme eğrilerinin elde edilmesi için başka bir yol olarak karşımıza çıkmaktadır.

Mevcut test sonuçları bu durumda sonlu elemanlar analizlerinin kontrolü için bir yol göstericidir. Bu da gösterir ki; bu analizler daha da ileri gidilerek tasarım denklemlerine adapte edilebilir. Bu tez 3-boyutlu doğrusal olmayan sonlu elemanlar analizleri ile köşebentlerle oluşturulmuş yarı rijit bağlantıların incelenmesini yapıp bunların test sonuçları ve farklı araştırmacılar tarafından geliştirilmiş matematiksel modellerle karşılaştırılmasını amaçlamaktadır.

Anahtar Kelimeler: Yarı-Rijit Çelik Kiriş Kolon Bağlantılar, 3-D Doğrusal Olmayan Sonlu Elemanlar Analizi, Yarı-Rijit Bağlantılar için Matematiksel Modeller

## **ACKNOWLEDGMENTS**

I wish to express my deepest gratitude to my supervisor and mentor Dr. Afşin Sarıtaş for his continuous support and advice throughout the thesis work.

I would also like to offer my thanks to each of my family member for their patience and support during my study.

The help of my friends and colleges are also acknowledged with great appreciation. Also I specially thanks to the teachers and faculty members during my educational life.



# TABLE OF CONTENTS

ABSTRACT .....	iv
ÖZ .....	vi
ACKNOWLEDGEMENTS .....	viii
TABLE OF CONTENTS .....	ix
LIST OF TABLES .....	xi
LIST OF FIGURES .....	xii
LIST OF SYMBOLS AND ABBREVIATIONS .....	xiv
CHAPTER	
1. INTRODUCTION .....	1
1.1 General .....	1
1.2 Connection Classification .....	2
1.2.1 Strength .....	3
1.2.2 Ductility .....	3
1.2.3 Stiffness (Connection Flexibility) .....	4
1.3 Types of Partially Restrained Connections .....	5
1.3.1 Single Web-Angle and Single Plate Connections .....	5
1.3.2 Double Web-Angle Connections .....	5
1.3.3 Top and Seat Angle Connection .....	6
1.3.4 Top and Seat Angle with Double Web-Angle Connections .....	6
1.3.5 Extended End Plate Connections and Flush End Plate Connections .....	6
1.3.6 Header Plate Connections .....	7
1.4 Historical Background of Finite Element Analysis of Semi-Rigid Connections .....	9
1.5 Objective and Scope .....	13

2. MODELING OF THE SEMI-RIGID CONNECTIONS WITH FINITE ELEMENTS .....	15
2.1 Detailed Modeling Approach towards Simulation .....	17
2.2 Previous Experimental Research.....	18
2.3 Finite Element Models .....	25
2.3.1 General Configuration for Finite Element Models .....	25
2.3.2 Element Types .....	26
2.3.3 Consideration of Friction and Pretension .....	28
2.3.4 Material Models .....	30
2.4 The Outputs of the Finite Element Analyses .....	34
2.4.1 The Results of the Top and Seat Angle Connection with Double Web Angles .....	34
2.4.2 The Results of the Top and Seat Angle Connection without Double Web Angles .....	43
3. MODELING OF THE SEMI-RIGID CONNECTIONS WITH FINITE ELEMENTS .....	48
3.1 Review of the Mathematical Models and Definitions .....	49
3.1.1 Linear Connection Model .....	49
3.1.2 Multi-linear Connection Model .....	50
3.1.3 Polynomial (Frye and Morris) Model .....	51
3.1.4 The Power Model .....	53
3.2 Comparison of Mathematical Models with Finite Element Analysis.	61
4. SUMMARY AND CONCLUSION .....	67
4.1 Summary .....	67
4.2 Conclusion .....	68
REFERENCES .....	71

## LIST OF TABLES

### TABLES

Table 2-1	Schedule of Test Specimens (Azizinamini <sup>[11]</sup> ) .....	21
Table 2-2	Schedule of Test Specimen Kukreti et al. <sup>[13]</sup> .....	24
Table 2-3	Mechanical Properties of the Used Specimens in the Experiment of Azizinamini <sup>[11]</sup> .....	31
Table 3-1	Standardization Constants for Frye and Morris Polynomial Model <sup>[5]</sup> .....	52

## LIST OF FIGURES

### FIGURES

Figure 1-1	Moment Rotation Characteristic of a Typical Semi-Rigid Connection .....	4
Figure 1-2	Typical Types of Semi-Rigid Connections .....	8
Figure 1-3	Portion of Flange Angle used in Azizinamini Finite Element Analyses .....	10
Figure 1-4	Finite Element model of Yang et al. ....	11
Figure 1-5	Finite Element model of Citipitioğlu et al. ....	12
Figure 2-1	A Sample Schematic Representation of the Azizinamini Test Setup .....	19
Figure 2-2	Geometric Variables for Top and Seat Angle Connection from Kukreti et al. Tests .....	23
Figure 2-3	A Sample Test Setup used by Kukreti et al. ....	24
Figure 2-4	A Typical Stress – Strain Diagram for Mild-Carbon Steel .....	30
Figure 2-5	A Sample Geometrical Representations of the Finite Element Models of Top and Seat Angle Connection with Double Web Angles .....	33
Figure 2-6	A Sample Geometrical Representations of the Finite Element Models of Top and Seat Angle Connection .....	33
Figure 2-7	Analysis Result and Comparison of the 14S1 Model .....	35
Figure 2-8	Deformed Shape of the 14S1 Finite Element Model .....	36
Figure 2-9	Analysis Result and Comparison of the 14S2 Model .....	37
Figure 2-10	Analysis Result and Comparison of the 14S3 Model .....	39
Figure 2-11	Analysis Result and Comparison of the 14S4 Model .....	40
Figure 2-12	Analysis Result and Comparison of the 14S5 Model .....	41
Figure 2-13	A Sample Deformed Shape of TS Connections .....	44
Figure 2-14	Comparison of the Test and Finite Element Analysis of TS5 Connection .....	44

Figure 2-15	Comparison of the Test and Finite Element Analysis of TS6 Connection .....	46
Figure 3-1	Size Parameters for the Top and Seat Angle Connections of the Frye and Morris Polynomial Model .....	52
Figure 3-2a	Deflection Configuration of Elastic Condition of the Connection .....	56
Figure 3-2b	Applied Forces in Ultimate State of the Connection .....	56
Figure 3-3a	Top Angle Connection Cantilever Beam Model of Ultimate Condition .....	56
Figure 3-3b	Mechanism of Top Angle at Ultimate Conditions .....	56
Figure 3-4	Mechanism of Web Angle Connection at Ultimate State .....	57
Figure 3-5	Seat Angle Connection .....	57
Figure 3-6	The Geometrical Parameters of Eurocode 3 Model .....	60
Figure 3-7	Comparison of 14S1 Specimen .....	62
Figure 3-8	Comparison of 14S2 Specimen .....	62
Figure 3-9	Comparison of 14S3 Specimen .....	63
Figure 3-10	Comparison of 14S4 Specimen .....	63
Figure 3-11	Comparison of 14S5 Specimen .....	64
Figure 3-12	Comparison of TS5 Specimen .....	64
Figure 3-13	Comparison of TS6 Specimen .....	65

## LIST OF SYMBOLS AND ABBREVIATIONS

2-D	Two Dimensional
3-D	Three Dimensional
AISC	American Institute of Steel Construction
ASTM	American Society for Testing and Materials
a, b	Curve Fitting Parameters
$C_1, C_2, C_3$	The Constants for the Polynomial Model
d	The Depth of the Beam Element
$d_b$	The Bolt Diameter
$d_1, d_2, d_3, d_4$	The respective depths of the Top and Seat Angle with Double web Angles Connection
E	Modulus of Elasticity
$EI_t$	The Bending Rigidity of the Top Angle
$EI_s$	The Bending Rigidity of the Seat Angle
$EI_a$	The Bending Rigidity of the Web Angles
$EI_{beam}$	The Bending Rigidity of the Beam
$e_t$	The Distance Between Bolt Center and the Edge of the Top Angle
FR	Fully Restrained
$F_{pretension}$	Applied Pretension Force
$g, g_c, g_b$	Gauge Distances for the Bolted Connections
$g_1, g_2, g_3, g_y$	The Defined distances for the Top and Seat Angle with Double web Angles Connection
K	Standardization Constant for Polynomial Model
k	Filler Length
L	The Length of the Beam
$l_v, l_h$	Vertical and Horizontal Length of the Angles
$l_{so}$	The Length of the Seat Angle without Filler
M	The Bending Moment
$M_p^{beam}$	The Plastic Moment Capacity of the Beam

$M_{pt}$	The Plastic Moment in the Top Angle
$M_{os}$	The Plastic Moment in the Seat Angle
$M_s$	The Reference Moment for Secant Stiffness
$M_u$	The Ultimate Moment Capacity of the Connection
$m_{ta}$	The Distance Between Plastic Hinges in Eurocode 3
$m_{ta}^*$	The Modified Distance Between Plastic Hinges
$n$	The Shape Parameter
PR	Partially Restrained
$R_l$	The Reference Stiffness for the Connection
$R_k$	The Stiffness of the Connection
$R_{ki}$	The Initial Stiffness of the Connection
$R_{kit}$	The Top Angle Contribution to Initial Stiffness of the Connection
$R_{kis}$	The Seat Angle Contribution to Initial Stiffness of the Connection
$R_{kia}$	The Web Angles Contribution to Initial Stiffness of the Connection
$R_{kp}$	The Plastic Connection Stiffness
$R_{ks}$	The Secant Stiffness of the Connection
$r_t$	The Filler Radius of the Top Angles
TS	Top and Seat Angle Connection
$t_t$	Thickness of the Top Angle
$t_s$	Thickness of the Seat Angle
$t_a$	Thickness of the Web Angles
$V_{ot}$	The Reference Shear Force in the Top Angle
$V_{oa}$	The Reference Shear Force in the Web Angle
$V_{pa}$	The Resultant of Plastic Shear Force in a Single Web Angle
$V_{pt}$	The Plastic Shear Force in the Vertical Leg of the Top Angle
$V_{pu}$	The Plastic Shear Force in the Web Angle
$w$	The Width of the Heavy Hex Nut
$\alpha$	The Stiffness Factor
$\Psi$	The Modification Factor for Faella et al. Model
$\lambda$	Rigidity Index
$\eta$	Fixity Factor
$\emptyset, \theta$	Rotation
$\emptyset_0$	Reference Plastic Rotation

$\theta_u$	Connection Rotation at the Ultimate Moment Capacity
$\theta_u^*$	The Value of the Rotation When the Moment Dropped 80% of the Ultimate Moment Capacity



# CHAPTER 1

## INTRODUCTION

### 1.1 General

Steel structures have to be connected through effective connections with certain energy dissipation capacities in order to resist against earthquake induced ground motions. Before the Northridge (1994) and Kobe (1995) earthquakes, designers and also the codes at that times were in favor of welded connections designed for forces coming from earthquake motions, where these connections have great moment capacities indeed. However, these types of connections failed in brittle manner after reaching their capacities, and this caused severe damage to buildings in these earthquakes [1, 2]. In the light of the observation of post earthquake scene, one of the learned lessons is that the moment capacities are not the only criteria for the structural connection in earthquake resistant steel structures. Together with the sufficient moment capacity, the connections should have energy dissipation capacities for successfully resisting earthquake forces in ductile manner, as well.

In the following decade after Northridge and Kobe earthquakes, structural steel codes together with seismic codes established new rules for connections. In this perspective, partially restrained connections or semi-rigid connections have been more recently cited in the codes. Moreover, they are also acknowledged as an economical way to accomplish better earthquake performance in steel frames [3]. However, being economical in steel frame design and good at energy dissipation for earthquake response does not automatically make these connections popular in practical design applications, since there is not enough analytical and experimental research on the response of these types of connections. Furthermore, complicated analysis procedure and not knowing the range of application of these types of

connections repel designers in practice. As a result of this uncertainty, designers approach steel framing connections as either fixed or pinned. But, both of these assumptions do not reflect the actual nonlinear behavior of the connections.

Nonlinear response of the connection behavior was first recognized in the early 1930's. Then, certain attempts have been undertaken ranging from simple linear and bilinear curves to more sophisticated polynomial and exponential models for reflecting actual nonlinear behavior of the connections [4]. These models are basically moment-rotation type relations, and they are simply curve fitted with available experimental data and used to represent the effect of connections in a steel frame. Nevertheless, lack of knowledge on the experimental data with different parameters does not allow researchers to characterize moment-rotation functions for each different connection set and type. Due to the increase in computational power in the last decade, finite element applications are used to obtain moment-rotation curves to reflect the effect of nonlinearity in the connection response. By the help of finite element programs, effects of different parameters on the connection behavior can be investigated.

In this chapter, to be more comprehensive, the range of application for semi-rigid connections together with connection types are going to be clearly defined by the help of the current code of practice at the beginning. Then literature review on the experimental and analytical work on connections is presented. Finally, objective and scope of thesis are given at the end of this chapter.

## **1.2 Connection Classification**

Specifications in design codes mainly draw boundaries to classify each connection types, and the classification between the connections depends mainly on the following three parameters:

- Strength
- Ductility
- Stiffness

The contribution of these parameters to the classification can be explained by the help of AISC Specification for Structural Steel Buildings (2005) specifications as follows:

### ***1.2.1 Strength***

The strength parameter is coming from the comparison of the beam strength with the connection that bounds the beam. If the beam strength exceeds the connection strength then the priority shifts from strength to ductility [5]. If  $M_u$  is defined as the capacity of connection and  $M_p^{\text{beam}}$  the plastic moment capacity of the beam, then the strength of the connection can be classified as follows;

- A connection is full strength (FS) if  $M_u \geq M_p^{\text{beam}}$
- A connection is partial strength (PS) if  $M_u \leq M_p^{\text{beam}}$
- A connection has no flexural strength if it has a capacity less than  $0.2 M_p^{\text{beam}}$

### ***1.2.2 Ductility***

The ductility of connection is very important parameter when deformations are considered in the connections, where this is the typical case in partial strength connections [5]. If  $\theta_u$  denotes the value of connection rotation at ultimate moment and  $\theta_u^*$  the value of rotation at the point where the moment has dropped to 80% of ultimate value, AISC Seismic Provision (2005) states the following;

- A connection in a special moment frame (SMF) is ductile if  $\theta_u^* \geq 0.04$  radians
- A connection in an intermediate moment frame (IMF) is ductile if  $\theta_u^* \geq 0.02$
- Otherwise connection is considered as brittle.

### 1.2.3 Stiffness (Connection Flexibility)

Since the nonlinear behavior of the connection manifests itself at low levels of load, AISC suppose the initial stiffness of the connection,  $R_{ki}$ , does not adequately represent connection response at service levels [5]. The secant stiffness,  $R_{ks}$ , is more indicative of low level, nearly linear, response. The secant stiffness, defined as  $R_{ks} = M_s/\theta_s$ , where  $M_s$  is a nominal force level, e.g.,  $M_s=2/3 M_u$ , and  $\theta_s$  is the corresponding rotation. To classify the connections with their stiffness properties, a factor  $\alpha=R_{ks}L/(EI)_{beam}$  is defined and classification is done accordingly as follows;

- A connection is fully restrained (FR) if  $\alpha>20$ ,
- A connection is partially restrained (PR) if  $2\leq\alpha\leq20$ ,
- A connection is simple if  $\alpha<2$

The definitions in above mentioned properties are presented in Figure 1-1

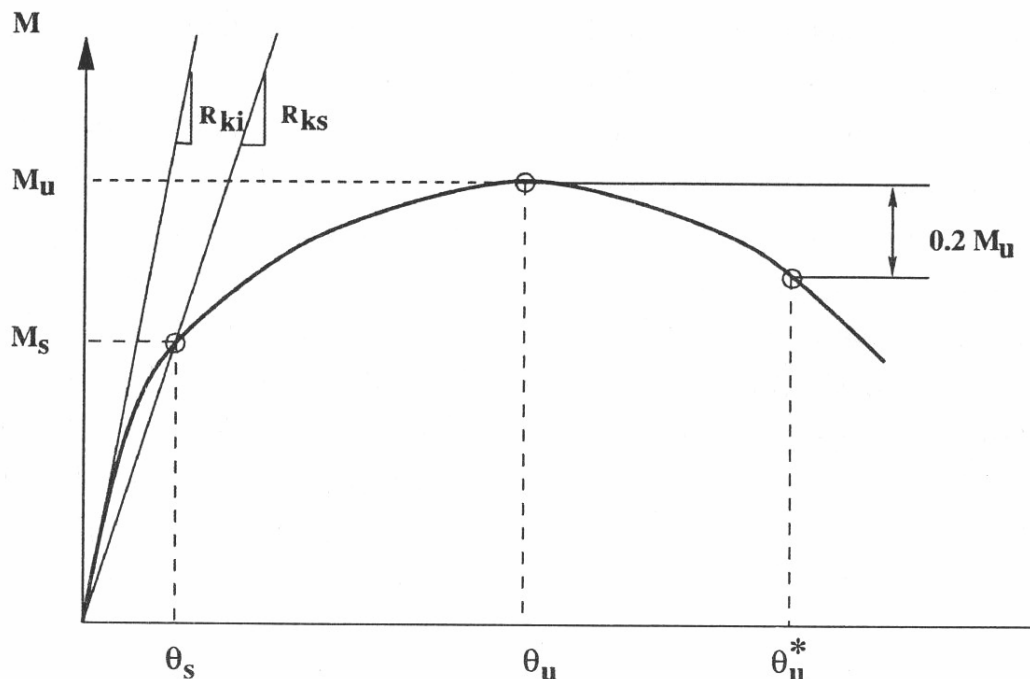


**Figure 1-1. Moment Rotation Characteristic of a Typical Semi-Rigid Connection**

### **1.3 Types of Partially Restrained Connections**

After defining the range of applicability with above mentioned procedure, let's proceed with the typical types of partially restrained beam-column connections.

#### ***1.3.1 Single Web-Angle and Single Plate Connections***

As represented in Figure 1-2a, a single web-angle connection composes of an angle bolted or welded to both the column and the beam web. If a single plate connection uses the plate instead of the angle, the material requisition of the connection will be less than a single web-angle connection (Figure 1-2b). It can be stated that the single web-angle connection has a moment rigidity equal about one-half of the double web-angle connection. On the other hand, the single plate connection has rigidity equal to or greater than the single web-angle connection since one side of the plate in the single plate connection is fully welded to the column flange [5].

#### ***1.3.2 Double Web-Angle Connections***

Figure 1-2c shows a double web-angle connection that composes of two angles bolted or riveted to both the column and the beam web. Earliest tests on double web-angle connections were conducted with rivets as fasteners by Rathbun (1936) [5]. After high strength bolts became popular around 1950's, the codes of specifications allow the usage of high strength bolts. Recently, high strength bolts replaced rivets in practical usage. The double web-angle connection is actually stiffer than the single web angle connection. However, the moment capacity of this connection type is one of the lowest among the other types. Therefore, this connection is considered as simple connection in practical analysis.

### ***1.3.3 Top and Seat Angle Connections***

The top and seat angle connection consists of two flange angles which connects the beam flanges with column flanges. Figure 1-2d shows the typical representation of such connections. In the AISC codes (ASD 1989) the sole purpose of the top and seat angle is explained as follows:(1) the top angle is used to provide lateral support to the compression flange of the beam and (2) the seat angle is used to transfer only the vertical shear and should not give a significant restraining moment on the end of the beam [5]. As indicated in the explanation the connection moment capacity is ignored by the code definition. Nevertheless, it is proven with the experimental results that this type of connections can transfer not only the vertical reaction, but also some end moment of the beam to column.

### ***1.3.4 Top and Seat Angle with Double Web-Angle Connections***

This type is a combination of top and seat angle and double web angle connection as shown in Figure 1-2e. Double web-angles provide an increase in the connection restraint characteristics of top and seat angle connections. This type of connections is generally referred as semi-rigid connection in many design specifications [5].

### ***1.3.5 Extended End Plate Connections and Flush End Plate Connections***

A typical end plate connection consists of an end plate welded to the beam end along both flanges and web in workshop and bolted to the column in the field. This type of connection usage has increased significantly since 1960 [5]. This type of connections is classified into two groups as an end plate either extended on the tension side only or extended on both tension and compression sides. These two types are shown in Figure 1-2f and 1-2g, respectively. Other than these, there is also flush end plate connection which covers the beam depth as shown in Figure 1-2h. The characteristic of transferring higher moments from beam to column makes

extended end plate connections fully restrained (FR) rather than partially restrained in most of the current code of specifications [5, 22, 42]. On the other hand, flush end plate connection is rather weaker than the extended end plate connection. The overall behavior of end plate connections is dependent on whether the column flanges act to prevent flexural deformation of the column flange and thereby influence the behavior of the plate and the fasteners [5].

### ***1.3.6 Header Plate Connections***

If the end plate connection does not cover the beam depth, this kind of end plate connections is called header plate connection which is shown in Figure 1-2i. The plate is welded to the beam and bolted to the column. The moment transfer capacity of this connection is similar to those of the double web-angle connection. As expected from this similarity, a header plate connection is used mainly to transfer the vertical shear of the beam to column instead of beam moment and generally categorized as simple connection.

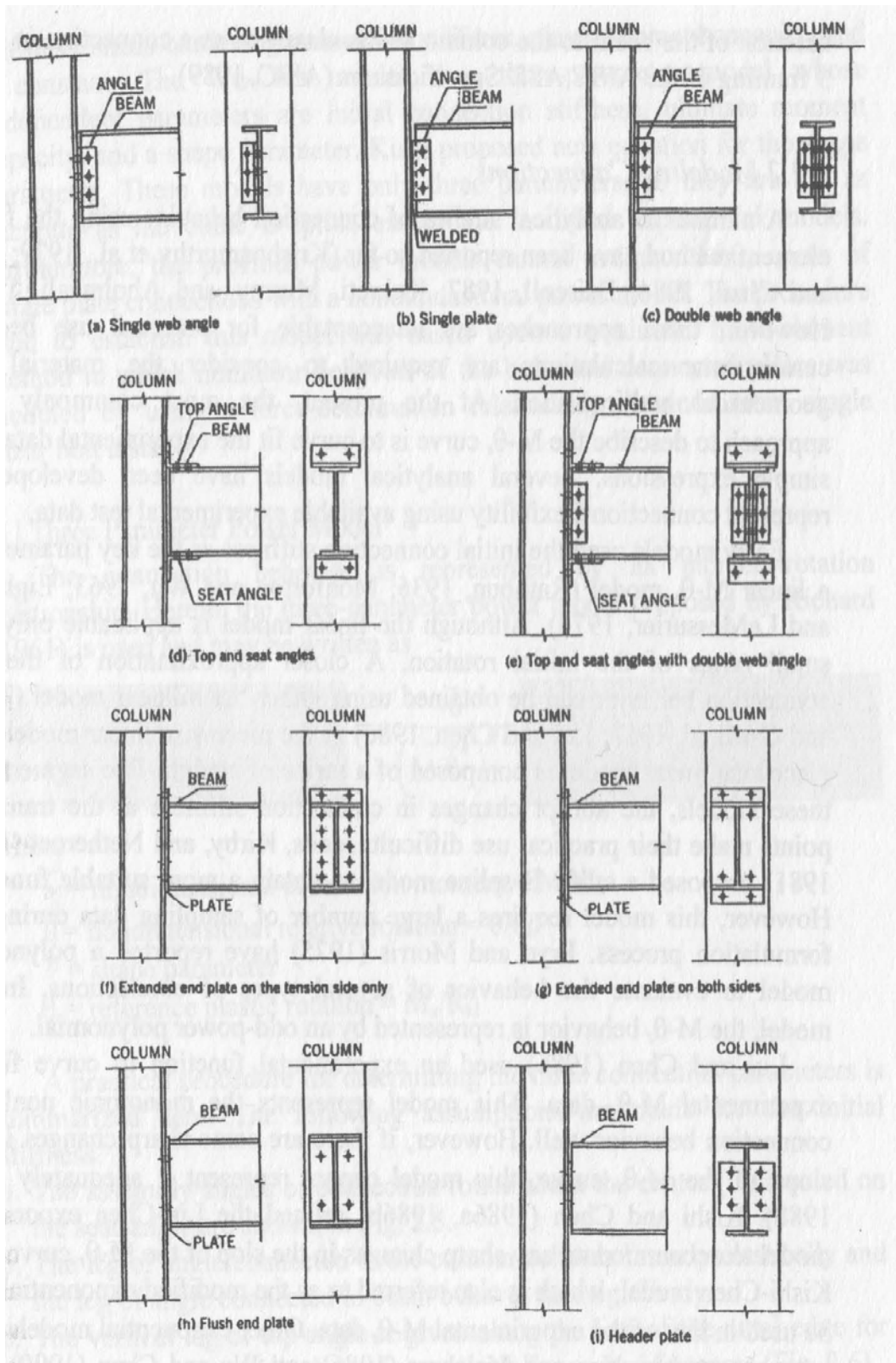


Figure 1-2. Typical Types of Semi-Rigid Connections [5]



## **1.4 Historical Background of Finite Element Analysis of Semi-Rigid Connections**

The use of nonlinear finite elements is one of the most effective modeling methods in representing connection response. Early attempts for modeling steel connections with finite elements were undertaken by Krishnamurthy in 1976. In this aspect, Krishnamurthy was also the pioneer in the field of 3-D modeling of bolted end plate connections. To model bolted end plate connections, eight-node sub-parametric bricks elements were used in Krishnamurthy's analysis [6, 7]. These analyses were linearly elastic but expensive, because contact was embodied artificially by attaching and releasing nodes at each loading step on the basis of the stress distribution. Due to the limited computer capacities, a correlation between two-dimensional (2-D) and three dimensional (3-D) finite element analyses was established and a parametric study was carried out with 2-D models [8]. After Krishnamurthy, developing 2-D finite element models for bolted connections became more popular among other researchers and, generally, a good agreement between analyses and experiments was observed. Indeed, 2-D displacement-based finite element models predict stiffer and stronger connection response compared to the corresponding 3-D models, unless both the connection displacement and stress fields are almost 2-D.

Recently, researchers used 3-D finite element models based on shell and contact elements in order to observe overall behavior of end plate together with beam and column flange [8]. The agreement between simulations and test data depends on how contact and beam elements simulate friction and bolt action, respectively. Along these, most of the finite element models were conducted by various simplifications and assumptions. In the finite element simulation attempts, friction between the connected bodies was generally ignored. Moreover, the geometries of the connecting bodies and the bolted parts are simplified in order to reduce the amount of computational effort.

Many researchers conducted analytical and experimental work on bolted end plate connections [4, 7-10]. On the other hand, there is little amount of analytical research on other types of steel connections (especially semi-rigid connections). Due to the limited amount of experimental analysis, numerical analyses with finite elements are also scarce in number for semi-rigid connections. One of the extensive and detailed experimental studies together with the finite element analysis was conducted by Azizinamini in 1985. In these tests, top and seat angles with double web angles connections were investigated. Furthermore, a finite element model was presented and the results of experimental data were compared with the analytical ones. In the finite elements models, a portion of the tension flange angle was modeled with 3-D elements as in Figure 1-3. Azizinamini used load-deformation curves obtained from the pull test together with 3-D finite element analysis and converted them into moment-rotation ( $M-\theta$ ) curves [11]. As can be seen from the figures, the 3-D analysis of the connections was simplified, since bolt holes and shanks together with friction between contact surfaces were rather ignored. Although finite element models of Azizinamini are old and simplified for the purpose of reducing computational effort, more recent attempts in analyzing the same tests have been undertaken by other researchers [4, 12]. More detailed investigation of Azizinamini's tests will be presented in the following chapters of this thesis.

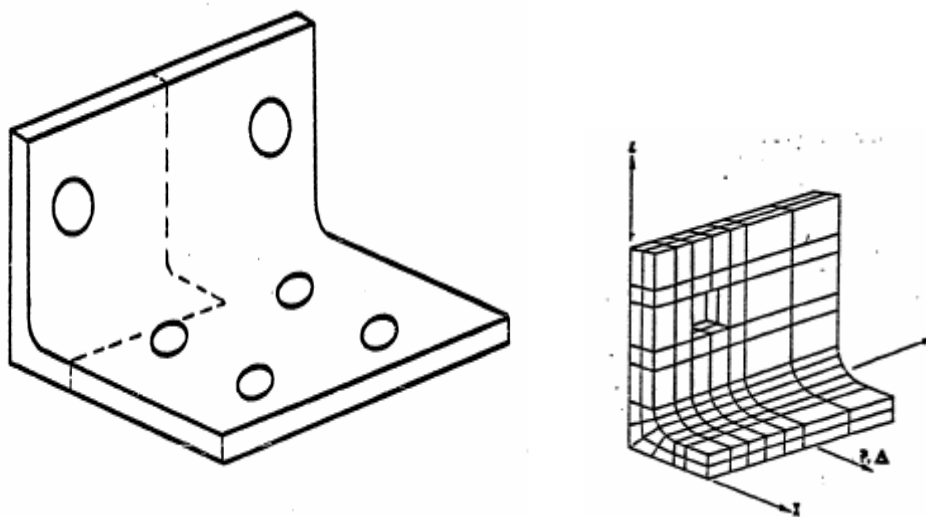


**Figure 1-3. Portion of Flange Angle used in Azizinamini Finite Element Analyses [11]**

Another experimental work on a different kind of semi-rigid connection was conducted by Kukreti et al. and published in 1999. In this analysis, top and seat angles without double web angles connections were investigated. This experimental research has not been compared with any finite element analysis yet. On the other hand, Kukreti et al. chose another way of comparison by curve fitting the test results in the following simplified mathematical models: the bilinear, elastoplastic, Ramberg-Osgood, and the modified bilinear models [13].

Next attempt on semi-rigid connection modeling with finite element analysis was performed by Yang et al (2000). In this research, Yang et al. used double web angles which are bolted to column flange and welded to beam web. The finite element model was defined with one of the web angle and symmetry was utilized. 3-D finite elements and wedge elements were used to represent bolts, angles and welds. Hex bolt heads and nuts were idealized as squares to simplify analysis. The contact and bearing interactions between the bolt shanks and bolt holes were neglected. On the other hand, contact between the bolt heads and the outstanding leg of the angle was included in the model [14].

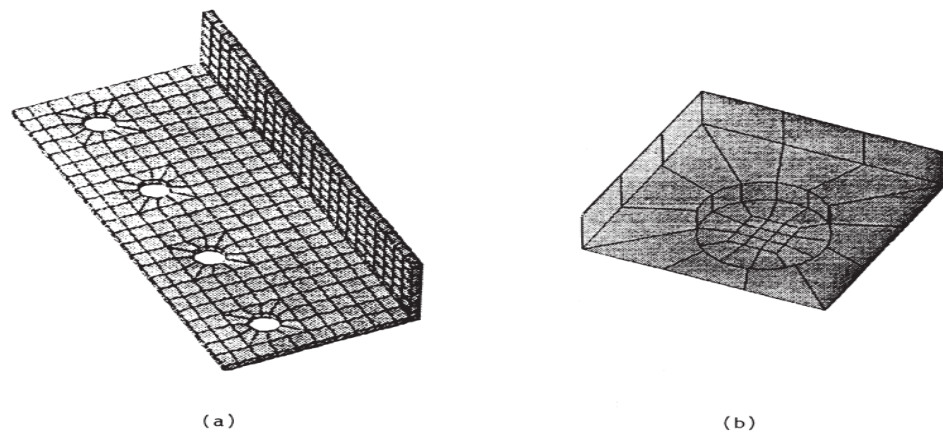


**Figure 1-4. Finite Element model of Yang et al. a) Web Angle, b) Bolt [14]**

Abolmaali et al. (2003) [15] conducted experiments with double web angle connections. In those tests, bolted connections were used for the beam web in addition to welded connections. Both types of connections were tested alongside with the older analysis of flush end plate connections and ductility of the mentioned connections was compared. Just like Kukreti et al. tests, these tests have not yet been analyzed with finite element analysis. Also there were neither any related mathematical model nor any curve fitted function presented.

More recent finite element analyses concentrate mainly on old but detailed test results, since conducting another test needs a great budget to spend. Among these analyses, two of them can be highlighted: Citipitioglu et al. (2001) [4] and Danesh et al. (2006) [12]. Both of these analyses focused on analyzing Azizinamini's test specimens. In these analyses, friction surfaces were modeled by using contact elements and bolts pretension was given with a calibration procedure which was either with thermal gradient or imposed deformation.

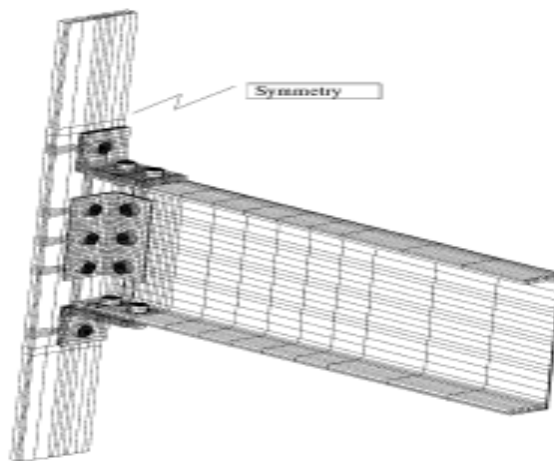


**Figure 1-5. Finite Element model of Citipitioglu et al [4]**

The current level of computational power and the advances made in finite element technology dictate more complicated and detailed finite element analysis for connection elements. The inclusion of contact bodies as well as bolt pretension, even slip critical connections are now modeled. On the other hand, the main problem of justification with test results remains unchanged.

## **1.5 Objectives and Scope**

In this thesis, finite element modeling of connections through 3-D solid finite elements is studied. The selected experiments for two distinctive semi-rigid connections are modeled with finite elements, namely the top and seat angles with or without double web angles connections. When available, the results of each case are compared with previous finite element analysis and mathematical models.

The thesis aims to use finite element analysis as a tool to obtain a response to the complex behavior of the selected types of semi-rigid connections. By doing this, this thesis will provide a useful path for the later structural analyses that consider these types of connections. Also the physical behavior of analyzed connections is compared with that observed from the finite element models as well as simplified mathematical models to give an insight to engineers that are interested in steel beam to column semi-rigid connection design.

To fulfill the desired goals, the thesis is divided into four chapters. Excluding the first chapter, i.e. Introduction, the other chapters are as follows: in Chapter 2 finite element implementation of selected semi-rigid connections will be presented. In this presentation, required information for finite element analysis is given in a neat form. Different models with certain parameters are investigated and calculated results for moment-rotation curves are shown with the comparison of experimental test results coming from different researchers.

The third chapter is dedicated for simplified mathematical models developed for semi-rigid connections and their comparison with the current study together with the experimental performance of the connections will be presented.

The last chapter of the thesis contains the summary and conclusion of the whole study and gives a brief discussion about possible future research directions on semi-rigid connections.

## CHAPTER 2

### MODELLING OF THE SEMI-RIGID CONNECTION WITH FINITE ELEMENTS

The use of solid finite elements is one of the most suitable methods for modeling connections. Several attempts were undertaken through last four decades to model semi-rigid connections with 3-D finite elements as explained in Section 1.4. Earlier models were highly simplified so as to reduce computational effort. Increasing computational power in the last decade enables to cope with more complicated models with ease. However, the improvement in computational power does not necessarily mean accurate simulations of the actual behavior of the connections.

Actually, drawing moment-rotation curves which represent the result of very complex interaction between connection elements requires the consideration of the following [15, 16]:

- Geometrical and material nonlinearities of the elementary parts of the connection
- Bolt pretension force and its response under general stress distribution
- Contacts between bolts and plate components: i.e. bolt shank and hole, bolt head or nut contacts
- Compressive interface stresses and friction
- Slip due to bolt to hole clearance
- Variation of contact zones
- Welds
- Imperfections i.e. residual stresses and so on

Recent finite element analyses consider nonlinearities both in geometry and material together with bolt pretension force, contact elements, friction and slip [4, 12]. On the other hand, covering imperfections and variation of contact zones require a level of refinement which is not yet attained.

Besides the above list of details, there are also other modeling approximations that have great influence on the finite element analysis, and these can be stated as follows:

- The used finite element program
- Considered element types
- Meshing of the elements
- Number of the finite elements that is used
- Definition of holes and fills
- Boundary conditions
- Representation of the environment (i.e., temperature, rate of loading etc.)

Although there are many considerations to be taken into account related with the simulation of the semi-rigid connection as listed above, the finite element method provides highly accurate results even when some simplifications to above mentioned considerations are introduced to the model. Meanwhile, simulation with finite elements takes considerable amount of time in spite of the improvement in the computational power. Knowing these and the capacity of the personal computers, the user of a finite element program should consider where to make simplifications carefully. Since even small changes of the above mentioned properties may cause significant differences in the results. Furthermore, responses of different kinds of connections and modeling considerations for these types are different, as well.

In this thesis, two types of connections, which are considered and cited as semi-rigid in the literature, are going to be simulated. These are top and seat angles with and without double web angles connections. In the following sections of this chapter, several explanations and details will be presented on how to deal with above



mentioned considerations and on the simplifications made for the top and seat angles with or without double web angle connections.

## **2.1 Detailed Modeling Approach towards Simulation**

The simulations of semi-rigid connections are done by utilizing displacement based 3-D finite element models. The geometry of the connection system and the positioning of the connection elementary parts together with holes and fills in the parts have to be also implemented towards simulation of a known connection. Furthermore, a program which can perform 3-D nonlinear finite element analyses by utilizing contact bodies and given mesh condition should be selected.

For this purpose, the ANSYS [18] Workbench Design Modeler module is selected for both implementing geometries of the bodies and defining contact surfaces. Moreover, the holes and fills in the bodies are also modeled by Design Modeler inside the bodies. On the other hand, the ANSYS Workbench Simulation module is activated for meshing of the elementary bodies of the connection parts. This module can recognize parts of the connection and has surface recognition. Each surface that connects with other surfaces can be defined in the simulation environment of the program. The analyses are also conducted within the simulation environment provided by the ANSYS Workbench simulation module.

The meshing of the composed bodies, i.e. beam element, bolts, angles and other mechanical bodies is done relative to their dimensions. By this way, the holes and fills which are defined and implemented by Design Modeler are perfectly meshed and introduced into simulation module. The relevance system also allows user to mesh each body and surface as defined in the Design Modeler part with exact geometry by not losing track of the connection between each body. These exact geometrical shapes include bolts, bolt heads and nuts. As a result of this modeling approach, simplifications introduced by other researchers (see Section 1.4) for the geometric bodies become unnecessary. Moreover, all the nodes created by the

meshing procedure are not susceptible to discrete bond between each finite element, since whole solid body is meshed continuously.

After these explanations, the experimental specimens chosen for finite element simulation are presented in the following section.

## **2.2 Previous Experimental Research**

In this part, previous experimental works conducted on the two types of semi-rigid connections that are taken into consideration in this thesis are investigated. These two types as indicated in previous sections are top and seat angle with double web angle connection, and top and seat angle without double web angle connection. There is little experimental work on the former connection type, where the first tests in literature were conducted by Rathbun in 1936 (2 specimens were tested). Several decades later Azizinamini [11] published his Ph.D. thesis on this type of connection in 1985, where he tested 20 specimens. Azizinamini also tested top and seat angle connection without double web angles, yet these tests were not presented adequately. As a result, only the top and seat angle with double web angle specimens of Azizinamini are considered for finite element analysis, where the test set-up is composed of a pair of beams which are connected through a stub column in the center. This configuration can be seen in Figure 2-1.

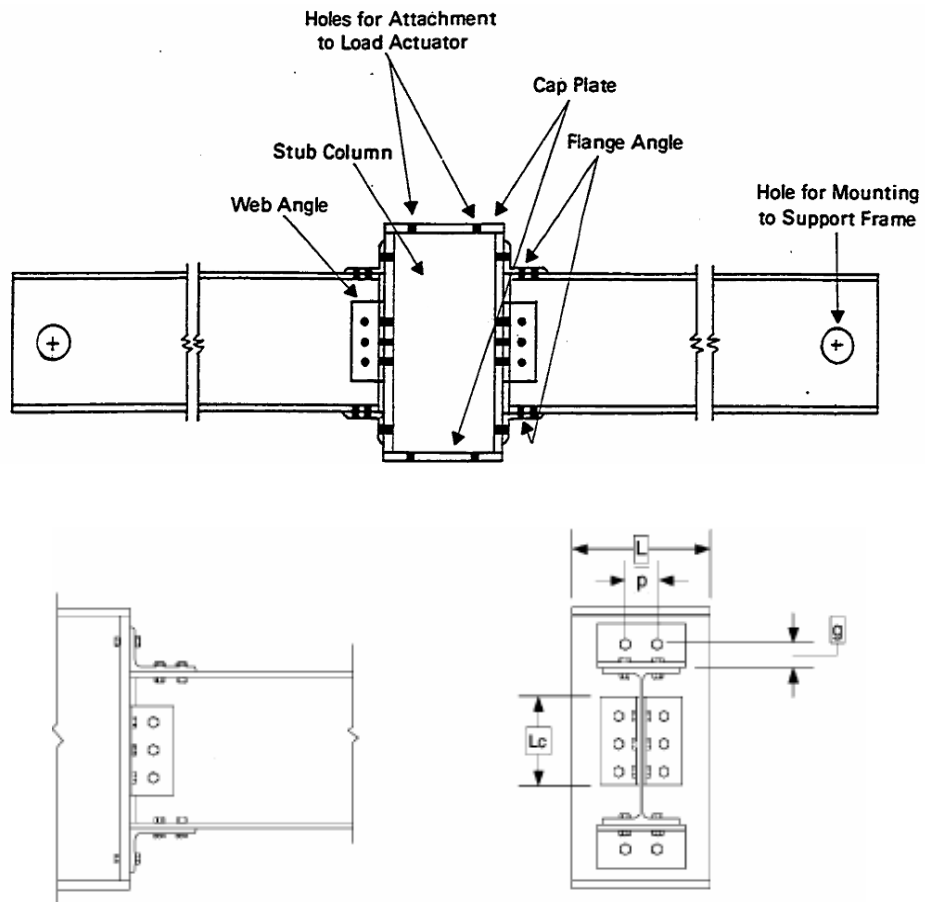


**Figure 2-1 A Sample Schematic Representation of the Azizinamini [11] Test Setup**

Azizinamini used two types of different configurations for top and seat angle connection with double web angles. In the first one, W12x96 (W305x144) stub column and W14x38 (W360x57) beams were used and angle thickness together with angle lengths were used as variables. In the second setup, W12x58 (W305x87) stub column and W8x21 (W203x32) beams were used and again angle thickness together with angle lengths were varied through experiments. Both of the test setups were used along with ASTM A325 heavy hex high strength bolts and nuts with ASTM A325 hardened washers. The diameters of the bolts were changed from test to test. Bolt spacing and bolt gages were also included in the investigated tests parameters. In the first test group including W14x38 (W360x57) beams, double web angles were connected to the stub column with three bolts (there was one exception in the 14S3 test setup which was connected with two bolts). Also, two set of bolts were used to

connect beam flange with flange angle and one set of bolts were used to connect flange angle to stub column. The other test group, which consisted of W8x21 (W203x31) beams was connected to stub column via two bolts in web angles. The configuration of the flange angles' connection did not change [11].

Azizinamini test setups were composed of relatively thick flanged stub column which ensured no or little plastic yielding through the testing process (for details of the column and beam sections as well as angles please refer the AISC Manual of Steel Construction [20]). Moreover, beams were also chosen so as to guarantee no plastic deformation occurred in the section. By this way, the failure had occurred in the connection before the beam element yielded or any plastic deformation occurred. As no plastic deformation was observed in the column and beam sections during testing, the same section was used through all tests. The effects of using the same beam and column elements were not presented and discussed in Azizinamini's research and by other researchers that analyzed his specimens through finite element method [4, 12].

The whole properties defining the experimental work conducted by Azizinamini are tabulated in Table 2-1. In this table, other than beam designation, length of top and bottom flange angles together with web angles, angle designations, gauge lengths and bolt spacing values are tabulated. The tabulated values are exported to the finite element analyses part as geometrical bodies for top and seat angle connection with double web angles.

**Table 2-1 Schedule of test specimens (Azizinamini [11])**

Specimen number	Bolt size (in. dia.)	Beam section	Angle Designation	Top and bottom flange angles			Web angles	
				Length (in.)	Gauge in leg on column flange <i>g</i> (in.)	Bolt spacing on column flange <i>p</i> (in.)	Angle Designation	Length (in.)
14S1	3/4	W14x38	L6x4x3/8	8	2 1/2	5 1/2	2L4x3 1/2 x1/4	8 1/2
14S2	3/4	W14x38	L6x4x1/2	8	2 1/2	5 1/2	2L4x3 1/2 x1/4	8 1/2
14S3	3/4	W14x38	L6x4x3/8	8	2 1/2	5 1/2	2L4x3 1/2 x1/4	5 1/2*
14S4	3/4	W14x38	L6x4x3/8	8	2 1/2	5 1/2	2L4x3 1/2 x3/8	8 1/2
14S5	7/8	W14x38	L6x4x3/8	8	2 1/2	5 1/2	2L4x3 1/2 x1/4	8 1/2
14S6	7/8	W14x38	L6x4x3/8	8	2 1/2	5 1/2	2L4x3 1/2 x1/4	8 1/2
14S7	7/8	W14x38	L6x4x1/2	8	2 1/2	5 1/2	2L4x3 1/2 x1/4	8 1/2
14S8	7/8	W14x38	L6x4x5/8	8	2 1/2	5 1/2	2L4x3 1/2 x1/4	8 1/2
8S1	3/4	W8x21	L6x3 1/2 x5/16	6	2	3 1/2	2L4x3 1/2 x1/4	5 1/2
8S2	3/4	W8x21	L6x3 1/2 x3/8	6	2	3 1/2	2L4x3 1/2 x1/4	5 1/2
8S3	3/4	W8x21	L6x3 1/2 x5/16	8	2	3 1/2	2L4x3 1/2 x1/4	5 1/2
8S4	3/4	W8x21	L6x6x3/8	6	4 1/2	3 1/2	2L4x3 1/2 x1/4	5 1/2
8S5	3/4	W8x21	L6x4x3/8	8	2 1/2	5 1/2	2L4x3 1/2 x1/4	5 1/2
8S6	3/4	W8x21	L6x4x5/16	6	2 1/2	3 1/2	2L4x3 1/2 x1/4	5 1/2
8S7	3/4	W8x21	L6x4x3/8	6	2 1/2	3 1/2	2L4x3 1/2 x1/4	5 1/2
8S8	7/8	W8x21	L6x3 1/2 x5/16	6	2	3 1/2	2L4x3 1/2 x1/4	5 1/2
8S9	7/8	W8x21	L6x3 1/2 x3/8	6	2	3 1/2	2L4x3 1/2 x1/4	5 1/2
8S10	7/8	W8x21	L6x3 1/2 x1/2	6	2	3 1/2	2L4x3 1/2 x1/4	5 1/2

\* Two bolts at 3 inch spacing, mounted on top two holes on stub column

As indicated before, Azizinamini also presented a series of pull tests for top and seat angle connection without double web angles. The results of pull tests were converted to force-deformation curves and eventually to moment-rotation curves by numerical methods. Since finite element method that is used in this thesis allows to directly calculate moment-rotation curves, Azizinamini's pull tests for top and seat angles without double web angles will not be used in this thesis.

On the other hand, the top and seat angle connections without double web angles are also tested by other researchers. This research was presented briefly in Section 1.4. The experiments conducted by Kukreti et al. were published in 1999, and they are selected for comparison with the finite element analysis in this thesis. The research composed of a series of tests that only included top and seat angles without double web angles. All the bolted top and seat angle connections in consideration were defined by the Kukreti et al. by the following parameters [13];

- The distance from the heel of the angle to the centerline of the first bolt rows in the column flange,  $g_c$
- The bolt diameter,  $d_b$
- The depth of the beam,  $d$
- The angle thickness,  $t$
- The length of the angle leg (vertical) of the top or seat angle connected to the column flange,  $l_v$
- The bolt gauges in the outstanding leg of the top or seat angle,  $g_b$
- The width of the top or seat angle,  $l$

The tests conducted by Kukreti et al. included typically a beam connected to a short column with bolted top and seat angle connection. The flange angles were connected to the column element with one row of bolts and were attached to the beam element with two rows. The used column section was W8x67 (W200x100) thick flanged profile. This was used again in order not to allow the column flange to go beyond yield stresses and limit the deformation of column flange so that no significant rotation occurs in this part. Kukreti et al. suggested this approach as a first

step toward formulization of moment-rotation curves, where this approach was also followed before by other researchers [19].

Two beam sections were used throughout the experiments of Kukreti et.al. These sections were W14x43 (W360x64) and W16x45 (W410x67) with a length of 38.5 in (978 mm). Kukreti et al. chose these beam sections to ensure a variation between the beam elements and to eliminate plastic deformations in the beam elements during testing. By this way, same beam sections were used throughout the tests, and inelastic behavior and eventually failure occurred only in the connection components.

The reference drawing for the variables Kukreti et al. used in the test setup is presented in Figure 2-2 and the overall test setup is shown in Figure 2-3. The properties of the test specimens are defined in Table 2-2 below (In this table, TS stands for top and seat angle). As seen in Table 2-2, there is no such value regarding  $g_b$  so these values used in tests are assumed to be standard values for the beam sections defined in the Manual of Steel Construction [20].

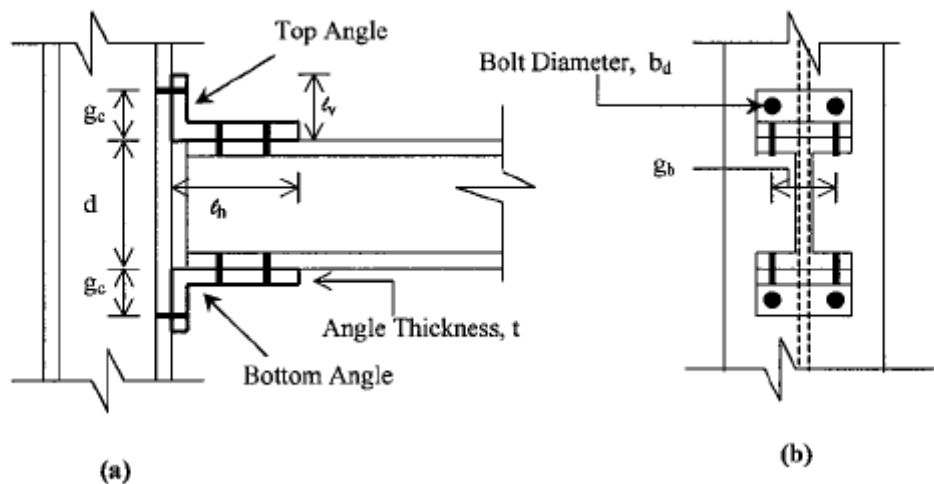


**Figure 2-2 Geometric Variables for Top and Seat Angle Connection from Kukreti et al. [13] Tests: a)Front View b)Side View**

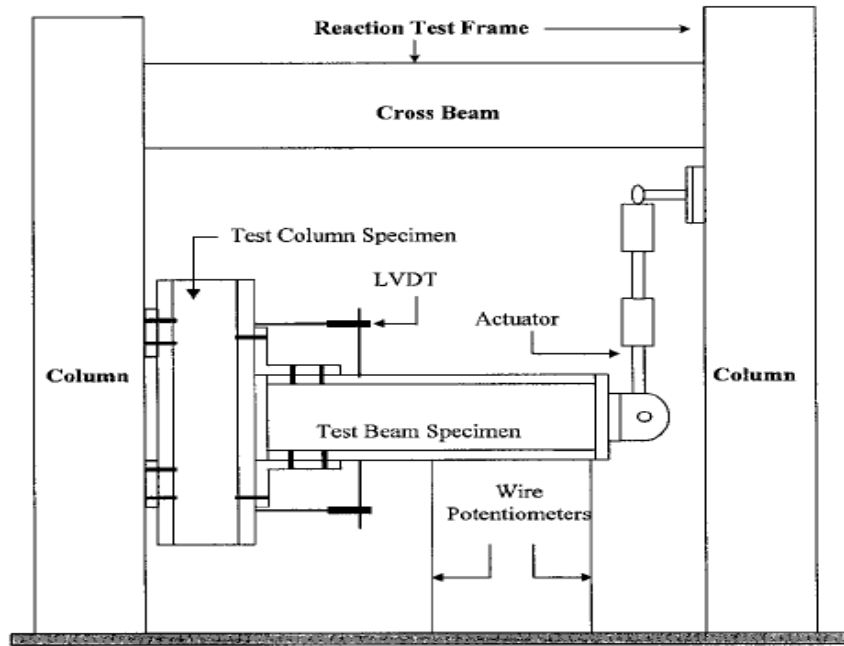


Figure 2-3 A Sample Test Setup used by Kukreti et al. [13]

Table 2-2 Schedule of Test Specimen Kukreti et al. [13]

Test number (1)	Test designation $TS - l_h \times l_v \times t \times d_b - g_c - d,$ [mm (in.)] (2)
1	$TS - 152 \times 102 \times 19 - 16 - 64 - 360$ ( $TS - 6 \times 4 \times 3/4 - 5/8 - 2.5 - 14$ )
2	$TS - 152 \times 152 \times 9.5 - 16 - 114 - 360$ ( $TS - 6 \times 6 \times 3/8 - 5/8 - 4.5 - 14$ )
3	$TS - 152 \times 152 \times 19 - 16 - 90 - 360$ ( $TS - 6 \times 6 \times 3/4 - 5/8 - 3.5 - 14$ )
4	$TS - 152 \times 152 \times 19 - 16 - 114 - 400$ ( $TS - 6 \times 6 \times 3/4 - 5/8 - 4.5 - 16$ )
5	$TS - 152 \times 102 \times 19 - 19 - 64 - 360$ ( $TS - 6 \times 4 \times 3/4 - 3/4 - 2.5 - 14$ )
6	$TS - 152 \times 102 \times 12.7 - 19 - 64 - 360$ ( $TS - 6 \times 4 \times 1/2 - 3/4 - 2.5 - 14$ )
7	$TS - 152 \times 102 \times 19 - 19 - 64 - 400$ ( $TS - 6 \times 4 \times 3/4 - 3/4 - 2.5 - 16$ )
8	$TS - 152 \times 102 \times 12.7 - 19 - 64 - 400$ ( $TS - 6 \times 4 \times 1/2 - 3/4 - 2.5 - 16$ )
9	$TS - 152 \times 152 \times 19 - 19 - 90 - 400$ ( $TS - 6 \times 6 \times 3/4 - 3/4 - 3.5 - 16$ )
10	$TS - 152 \times 102 \times 19 - 22 - 64 - 400$ ( $TS - 6 \times 4 \times 3/4 - 7/8 - 2.5 - 16$ )
11	$TS - 152 \times 152 \times 19 - 22 - 64 - 400$ ( $TS - 6 \times 6 \times 3/4 - 7/8 - 2.5 - 16$ )
12	$TS - 152 \times 152 \times 19 - 22 - 114 - 400$ ( $TS - 6 \times 6 \times 3/4 - 7/8 - 4.5 - 16$ )

In this thesis, Azizinamini tests from 14S1 to 14S5 and Kukreti et al. tests of TS5 and TS6 are selected for comparison with finite element analyses.



## **2.3 Finite Element Models**

The finite element models are prepared by using displacement-based nonlinear 3-D solid finite elements in order to simulate the inelastic behavior of a semi-rigid connection. In the following, the finite element models will be presented with detailed description, where an introduction was presented in Section 2-1 in this thesis. The experimental researches selected for finite element analyses were also discussed in Section 2-2.

### ***2.3.1 General Configuration for Finite Element Models***

The simulations of each selected semi-rigid connections are modeled with respect to original test setup procedure as far as the capability of the finite element program allowed. As mentioned before, Azizinamini's 14Sx tests [11] are modeled for the sake of the simulation of top and seat angle connections with double web angles. In the Azizinamini's tests, half of the overall test setup is modeled by the help of symmetry about the other half. The modeled part consists of a beam element, top and seat angles, web angles, bolts, nuts and column flange in this test setup.

The beam element is modeled as defined in the manual of Steel Construction [20]. The fills of the rolled section are also included to the beam sections. The bolt holes coming from flange angles are included in the beam definition to avoid further collision between the bodies.

The ASTM A325 heavy hex bolts are defined as described in the Specification for Structural Joints Using ASTM A325 or A490 Bolts from Research Council on Structural Connection [21]. The heads of the bolts are discretized as hexagonal shape with given dimension. The method of averaging of the bolt head diameter by simplifying it as a cylindrical body as done by previous researchers [4] is avoided by doing this. By using the same approach, the nuts are modeled as described on the specification [21]. The bolt holes are represented with 1/16 in (0.15875 cm) greater than the bolt shaft diameter. Although, this value is specified in the AISC code

Section J3 [22] as standard bolt holes diameter, there was no comment provided on the issue of bolt diameter in the Azizinamini's tests records.

Only the column flange part is modeled in the connection simulation. This is utilized since the column flange stiffness is great enough to accompany this part as stiff as a rigid connection. So the flange part of the column is modeled as fixed against deformations. Then, the bolts are placed in the flange part of the column according to tests configuration.

On the other hand, for the top and seat angle connections without double web angles tests by Kukreti et al. [13], the beam element, column flange, flange angles, bolts and nuts constructs the overall connections. Similar procedure from the previously explained Azizinamini's tests is followed for bolt heads and nuts as well as the beam and column definition with holes and fills. However, since the web angles are omitted in these models, the definitions for the web holes in the beam and the flange holes in the column are also omitted.

### ***2.3.2 Element Types***

The simulation of the connection elements are constructed from ANSYS SOLID 187 type 3-D higher order 10 nodes elements which possess a quadratic shape function for the displacement field, where these elements are well suited for the modeling of irregular meshes. The element is defined by 10 nodes having three degrees of freedom at each node: translations in the nodal x, y, and z directions. The element has plasticity, hyperelasticity, creep, stress stiffening, large deflection, and large strain capabilities together with mixed formulation capability for simulating deformations of nearly incompressible elastoplastic materials, and fully incompressible hyperelastic materials [18]. Using finite elements with quadratic displacement behavior for 3-D nonlinear finite element analysis is considered to be the best choice among other types of solid elements [23]; therefore the element type SOLID187 is suitable for the simulation of semi-rigid connections in this thesis.

In the connection models, the number of elements used in a connection model changes from one test setup to another. Approximately 14500 elements and 33500 nodes are used for each of Aziznamini's 14Sx specimens. On the other hand, an average of 8200 elements with approximately 19000 nodes build up each of Kukreti et al. specimens.

Another important aspect to consider is contact regions between the elementary parts. These contact regions include interaction between beam element and flange angles, bolt shank and bolt hole, bolt head and the part bolt head is attached, and furthermore the column flange and the angles that are attached to the column flange. The bolts can be assumed as clamped to the connection elementary part that bolts head and nut are attached, because the clamping forces produce enough strength to not allow bolt head and nut to move. Other than these clamped surfaces, simulated interactions have to consider the friction forces and the slip. These properties have great influence on the response of a modeled connection.

In the connection simulations, ANSYS CONTA174 and TARGE170 contact and target elements are used in order to take into account the forces due to the friction values and the deformation pattern due to slip. The element CONTA174 is capable of representing contact and sliding between 3-D target surfaces, which are TARGE170 element in this simulation environment, and a deformable surface, defined by this element. The element is applicable to 3-D structural and coupled field contact analyses. This element is located on the surfaces of 3-D solid or shell elements with mid-side nodes. CONTA174 has the same geometric characteristics as the solid or shell element face with which it is connected. Contact occurs when the element surface penetrates one of the target segment elements on a specified target surface. This element allows the usage of Coulomb and shear friction between the surfaces with a friction coefficient. This element also allows separation of bonded contact to simulate interface delamination. This is required for the slip condition to occur during the loading stage. On the other hand, TARGE170 element can describe various 3-D target surfaces for the associated contact elements. The contact elements themselves overlay the solid, shell, or line elements describing the boundary of a deformable body and are potentially in contact with the target surface, defined by

TARGE170. One can impose any translational or rotational displacement, temperature, forces and moments on target elements [18].

Other than contact surfaces, there are also a requisition of another element type for the pretension of bolts. The ANSYS Workbench module is used with the element type PRETS179 for the pretensioning of bolts. It is defined to be used in a 2-D or 3-D pretension section within a meshed structure with an imposed value of pretension. The element PRETS179 has one translational degree of freedom which lets the user to give only one directional pretension [18]. This is the last element type defined for the simulation of each test setup.

### ***2.3.3 Consideration of Friction and Pretension***

Friction value is one of the most important factors that affect both slip and the moment-rotation response of the connection. Taking into consideration of this fact, the friction value that a connection sustains has to be well defined. However, previous research based on the experiments such as Azizinamini [11] and Kukreti et al. [13] did not include the frictional effects resulting from the interaction of the main bodies. In these tests, there was no suggestion about the friction value or surface data. Without these conditions, the only remaining option is the use of current code of practice as a guide for analysis. Since both researches conducted their experiments by using American code of practice, the current code could help us in this respect. In current AISC manual (2005), there are two classes for defining faying surfaces and corresponding mean friction coefficient as follows [24]:

- Class A: This class denotes unpainted, mill scale or surfaces with Class A coatings on blast-cleaned steel surfaces. In this class mean friction coefficient,  $\mu$ , is defined as equal to 0.35.
- Class B: This class surfaces are unpainted blast-cleaned steel surfaces or surfaces with class B coatings. In this class mean friction coefficient,  $\mu$ , is defined as equal to 0.5.

These definitions for faying surfaces as well as mean friction coefficients all depend on how well the conditions of surfaces in the definition are satisfied. Since there is no assurance about the surfaces, the mean friction coefficient is possibly below the value just stated and it should be also varied from test to test. As an exemplification, the friction coefficient was varied between 0.255 and 0.50 in the analyses of Azizinamini's specimens in a previous research [4]. In this thesis work, the previous analyses are well appreciated and the friction values are used as defined in the current code of practice instead of using a series of friction values whose effect has already been known and described [4, 12].

When it comes to pretension, there is no information present in the research of Azizinamini's tests about applied pretension force [11], where the author mentions only the method of pretensioning. The test setups were prepared by tightening the bolts with an air wrench using the turn of the nut method [4, 11]. The other research, which Kukreti et al. conducted, specify the pretension value as equal to their proof load. The common values taken from the current code of practice defines the pretension values as follows [22, 24]:

- For the ASTM A325 3/4 in.(19.1 mm) bolts,  $F_{\text{pretension}}=28$  kips (124 kN)
- For the ASTM A325 7/8 in.(22.3 mm) bolts,  $F_{\text{pretension}}=39$  kips (173 kN)

These values are used in the finite element models to account for tightening effect in this thesis. As a matter of fact, the above mentioned values are only estimates for the real effects of pretension forces. By the way, the pretension forces also affect the frictional forces along the main surfaces of the bodies in contact. To see the effects of the pretension force the value of the force applied can be considered as a variable in the analysis. However, considering the frictional forces and the pretension values as both variables leads the models into a complex loop. Therefore, the friction coefficients and the pretension forces are used as constants described in the current code of practice (AISC 2005), and these are considered as constant during the finite element analyses of this thesis.

### 2.3.4 The Material Models

The material definitions take an important role in finite element analysis, where each definition for different parts of a connection should be carefully thought, i.e. the main connection elements, such as beam, column, flange and web angles, bolts and nuts, must be all simulated with appropriate material parameters and models. In this regards, the main dilemma is whether the simulated materials represent the actual test setup or not.

As a fact, the mild carbon steel ASTM A36 used in the analyses of both Azizinamini [11] and Kukreti et al. [13] can have different stress-strain diagrams by applying different loading rates and temperature. The temperature is not measured by the researchers as mentioned before. On the other hand, loading rate is a defined property by the experimental research considered for analysis in this thesis, where the rate of the loading of the investigated connections are related with the monotonic loading case, and steel takes the lower yield point and almost follow the exact path of the stress-strain diagram found in any steel design handbook. The figure that explains the regions of such stress strain diagram is provided in Figure 2-4 for convenience.

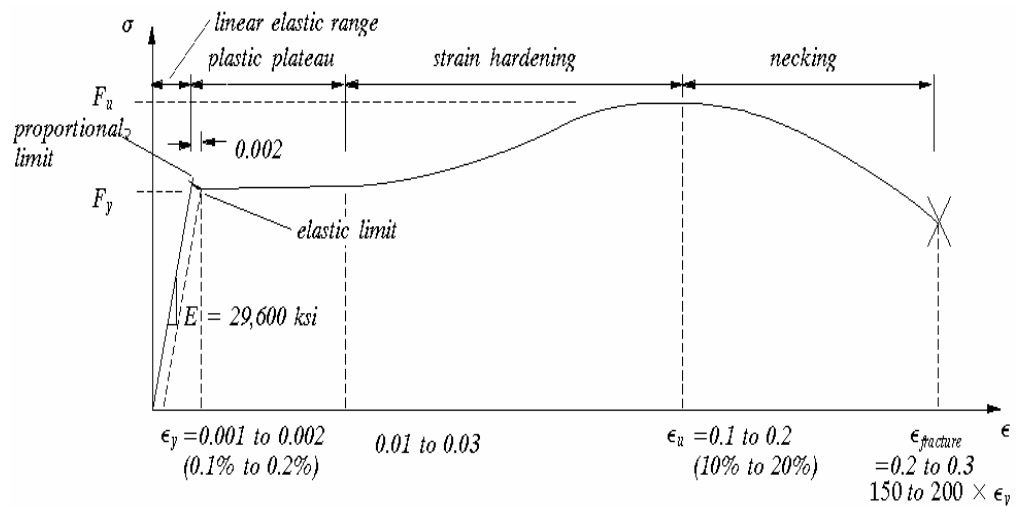


**Figure 2-4 A Typical Stress – Strain Diagram for Mild-Carbon Steel**

The given diagram is just a path that should be converted to a material model in a finite element model. The response in Figure 2-4 requires the definition of a function for each continuous region of the stress-strain diagram, resulting in a decrease in convergence rate and possibly localization of plastic strains at the corners of the bolt head [4]. In order to overcome the convergence problem, the material model for steel can be simplified. The same procedure was also preferred before by other researchers that conducted similar finite element analyses [4, 11, 12]. Moreover, it is reported that there is no significant change in the overall response of the connection due to such simplifications [4], where this is true as long as the connection response is confined to monotonic response.

The important parameters that are required for the definition of stress-strain diagram for steel are yield stress, ultimate stress, modulus of elasticity and tangent modulus. These parameters should be found out from the coupon tests as in the case of the experimental data of Azizinamini [4, 11], where these values are presented in Table 2-3. For the experimental research conducted by Kukreti et al., there is no information provided with regards to the properties of the used ASTM A36 steel in the experiments.

**Table 2-3 Mechanical Properties of the Used Specimens in the Experiment of Azizinamini [11]**

Designation	Mechanical Properties		
	Yield Stress (ksi)	Ultimate Strength (ksi)	Elongation in 2-inch Gage Length (percent)
ASTM A36	42.8	69.9	23.8
	42.9	67.9	22.9
	39.3	68.0	32.5
	37.6	67.9	31.9
	53*	80*	- -
	36.5	71.9	31.5
	43.7	69.9	31.3
	40.0	64.0	34.4
	38.0	66.0	37.5

\* Flange angle material, specimen 14S2.

In light of the above mentioned values, a bilinear material model is considered for the stress-strain relations of 3-D steel, and the properties of the steel used in the current finite element analyses in this thesis are chosen as follows:

- Modulus of elasticity,  $E_{\text{steel}}=30000$  ksi (207218 MPa),
- Yield stress of A36 steel,  $F_{\text{yield}}=36$  ksi (248 MPa)
- Ultimate Stress of A36 steel  $F_{\text{ultimate}}= 70$  ksi (483 MPa)
- Tangent Modulus of A36 steel  $E_t=180$  ksi (1241 MPa)
- Yield stress of Bolts,  $F_{\text{byield}}=92$  ksi (634 MPa)
- Ultimate Stress of Bolts  $F_{\text{bultimate}}= 120$  ksi (827 MPa)
- Tangent Modulus of Bolts  $E_{\text{bt}}=558$  ksi (3845 MPa)

The materials defined in the ANSYS Workbench platform with bilinear curves are converted to 3-D material properties with inside routine of the program just like  $J_2$  plasticity case in other programs i.e.: Opensees, Abaqus.

The finite element meshes of a top and seat angle with and without double web angles connection considered for analysis in thesis are presented in Figures 2-5 and 2-6, respectively.



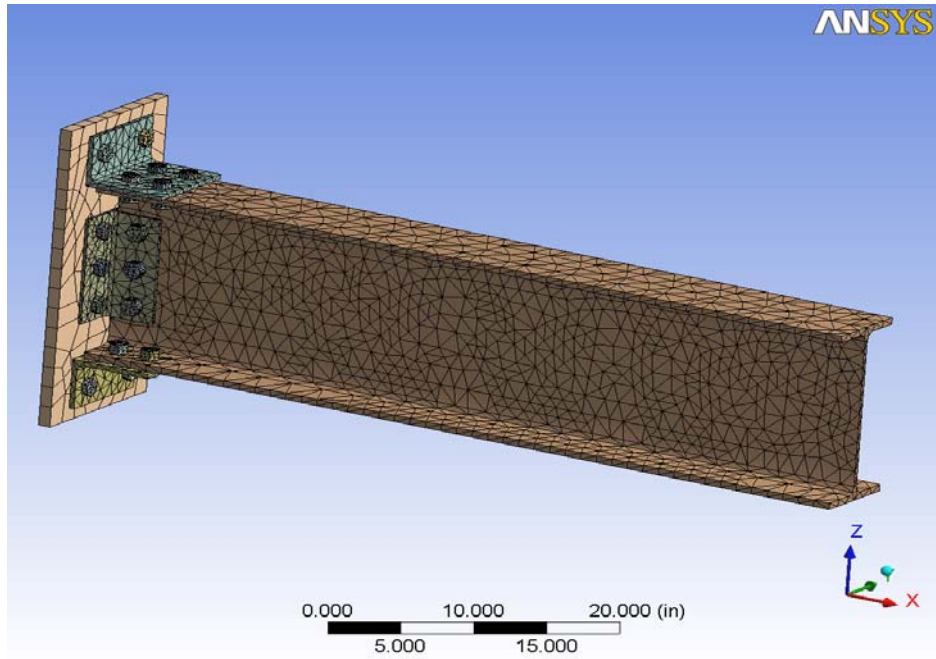


**Figure 2-5 A Sample Geometrical Representations of the Finite Element Models of Top and Seat Angle Connection with Double Web Angles**

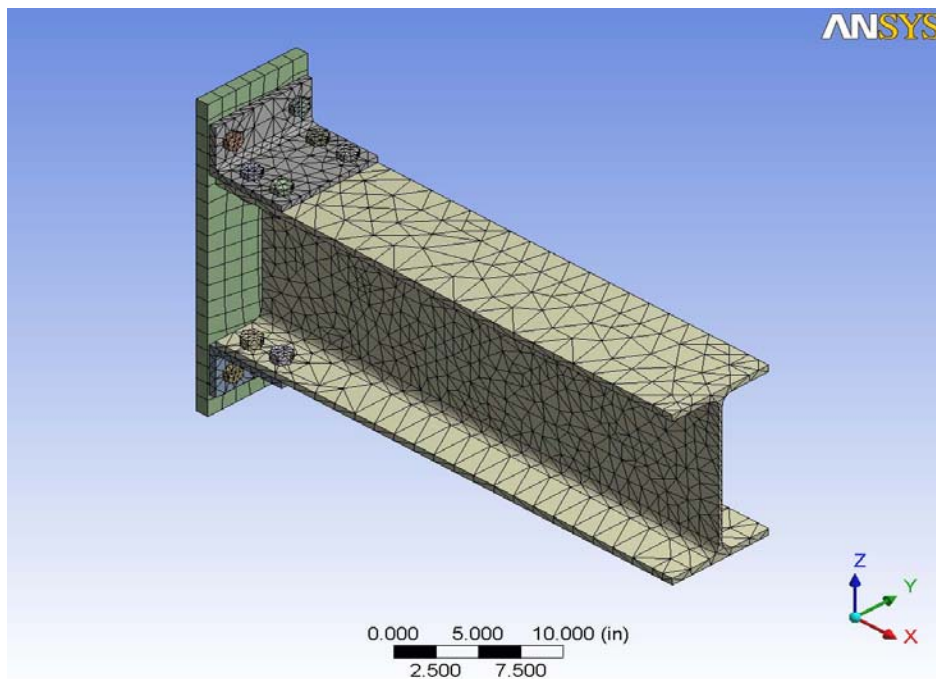


**Figure 2-6 A Sample Geometrical Representations of the Finite Element Models of Top and Seat Angle Connection**

## **2.4 The Outputs of the Finite Element Analyses**

In previous sections, all the necessary descriptions for the nonlinear 3-D finite element analysis of top and seat angle connection with or without double web angles were discussed in detail. In this section, the results from the analysis will be presented and compared with the experimental data and other finite element simulations performed in literature. The discussion of the results will be also presented. First, the finite element results from the analysis of top and seat angle with double web angle connection specimens by Azizinamini[11] are presented, and then the specimens tested by Kukreti et al.[13] are considered for the comparison of the response of top and seat angle without double web angle connections.

### ***2.4.1 The Results of Top and Seat Angle Connection with Double Web Angles***

Azizinamini's 14S1 to 14S5 connection specimens are selected for comparison of the response for top and seat angle connections with double web angles. The properties of these models were defined previously in Table 2-1. The main frame of the outputs of each analysis consists of comparison of the analytical and experimental results. Five different finite element models are prepared for the representation of corresponding Azizinamini test specimens.

Let's begin with the 14S1 model that is composed of W14x38 (W360x57) beam, L6x4x3/8 (L152x102x9.5 mm) top and seat angle, L4x3<sup>1/2</sup>x1/4 (L102x89x3.6 mm) web angles with 3/4 in (19.1 mm) bolts. The model was built up by considering a pretension value of 28 kip (124 kN) as discussed in Section 2.3.3. The corresponding friction coefficient value for the faying surfaces are selected as the typical value of a type A connection, where  $\mu=0.35$  [24]. The result of the finite element analysis of this specimen is presented in Figure 2-7.

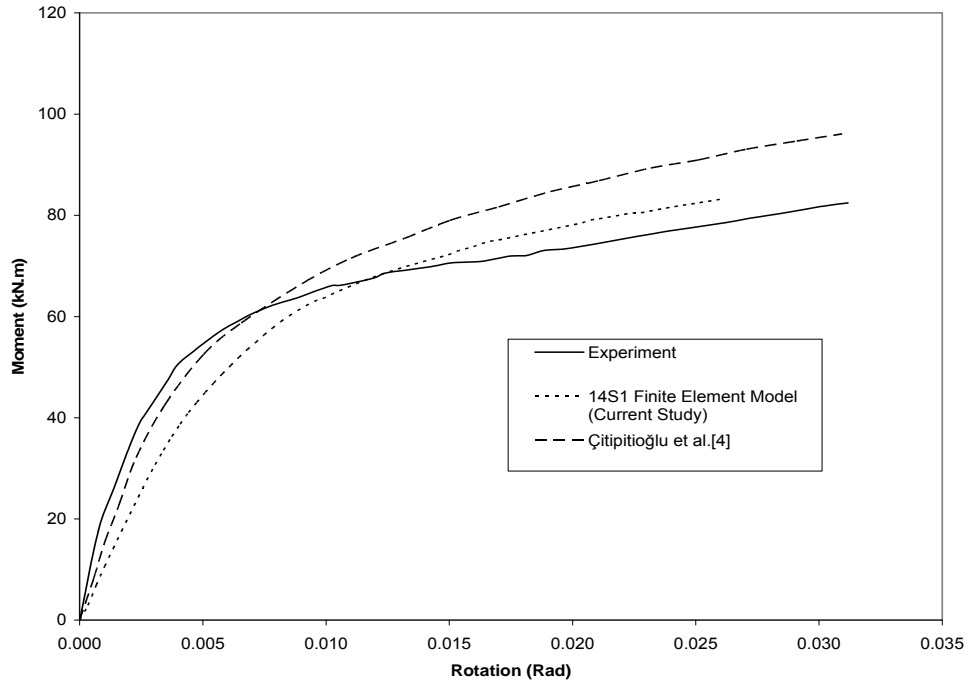


**Figure 2-7 Analysis Result and Comparison of the 14S1 Model**

The results show that the initial stiffness value is estimated below the experimental analysis. The fact that there are several uncertainties inherent in a test specimen and setup should also not be forgotten i.e.: the yield strength could vary even for the same steel material and the variations for the modulus of elasticity, and residual stresses are also common in steel members. Despite the error in the initial stiffness, the nonlinear response from the finite element analysis of the connection follows the same tangent as the experimental one, and this suggests the fact that the tangent modulus of both A36 steel and A325 bolts are estimated correctly. Moreover, the selected friction value and pretension forces are also in the correct range of application. In Figure 2-7, the analytical response in the nonlinear range of the current study is overestimated with respect to the experimental one since the yield values are different between the test specimen and the analytical model. In Figure 2-8, the deformed shape obtained from the analysis shows a correct pattern, and this proves that a correct approach is followed for the modeling of the top and seat angle with double web angles connection. This figure is a sample for all the simulated 14Sx connections, where all 14Sx specimens has 3 bolts in the web region except than 14S3 which has 2 bolts.

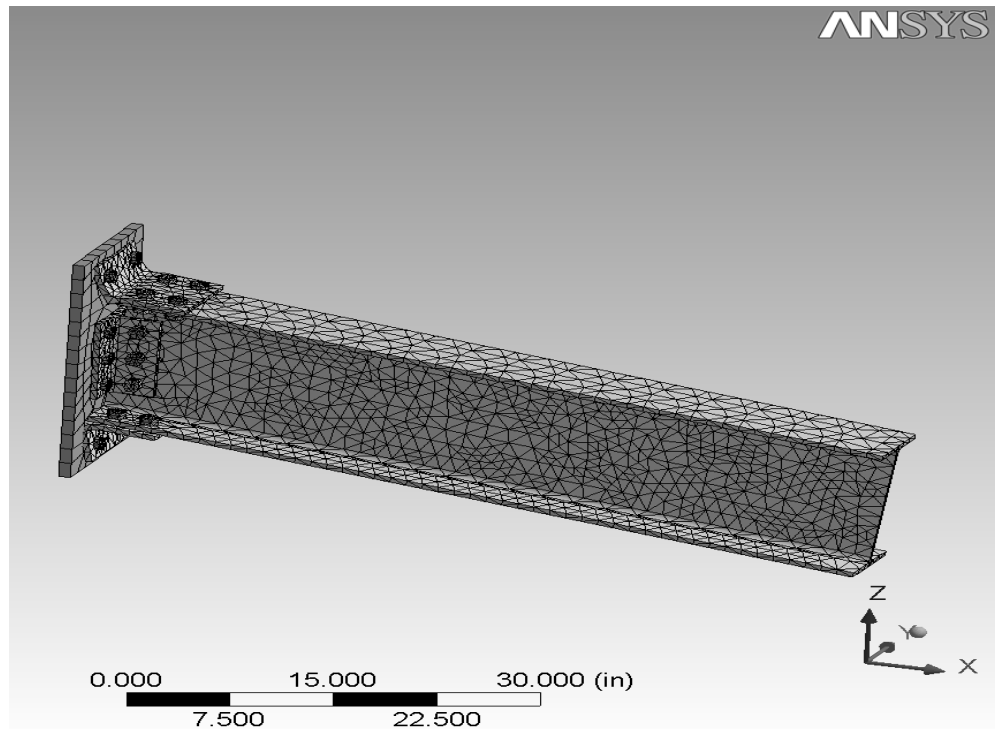


**Figure 2-8 Deformed Shape of the 14S1 Finite Element Model**

The current finite element analysis is also compared with the analysis conducted by Citipitioglu et al.[4] in Figure 2-7. While the current study uses yield strength value for A36 steel as suggested in design codes, Citipitioglu et.al. used a higher yield strength value for the same steel. In the figure, the initial stiffness obtained from Citipitioglu’s analysis is bigger than the current analysis. While the initial stiffness obtained in this study is on the safe side, the nonlinear response from Citipitioglu’s analysis overestimates the response. The difference in the nonlinear range might be caused due to the fact the current approach uses a 3-D higher order 10 nodes brick element that possess a quadratic displacement behavior while the other finite element model used 8-node brick elements with constant displacement field. The differences between the two finite element analyses can be summarized as follows: better approximation of the initial stiffness leads to a loss of accuracy in response for the ultimate moment and the slope of the nonlinear response.

Moreover, the use of smaller tangent modulus that are picked from the range of A36 steel and A325 bolt steel data seem to be beneficial for the sake of the nonlinear part of the connection behavior.

The next simulation is 14S2 test specimen, where this connection consists of W14x38 (W360x57) beam, L6x4x1/2 (L152x102x12.7 mm) top and seat angle, L4x3<sup>1/2</sup>x1/4 (L102x89x3.6 mm) web angles with 3/4 in (19.1 mm) bolts. The simulation is performed under the condition of 28 kip (124 kN) pretension value together with a friction coefficient  $\mu=0.35$ . The connection, as seen from its properties, is supplied with greater flange angles where the other properties remain the same as the first test specimen (14S1). The result of the finite element analysis from current study is presented in Figure 2-9.

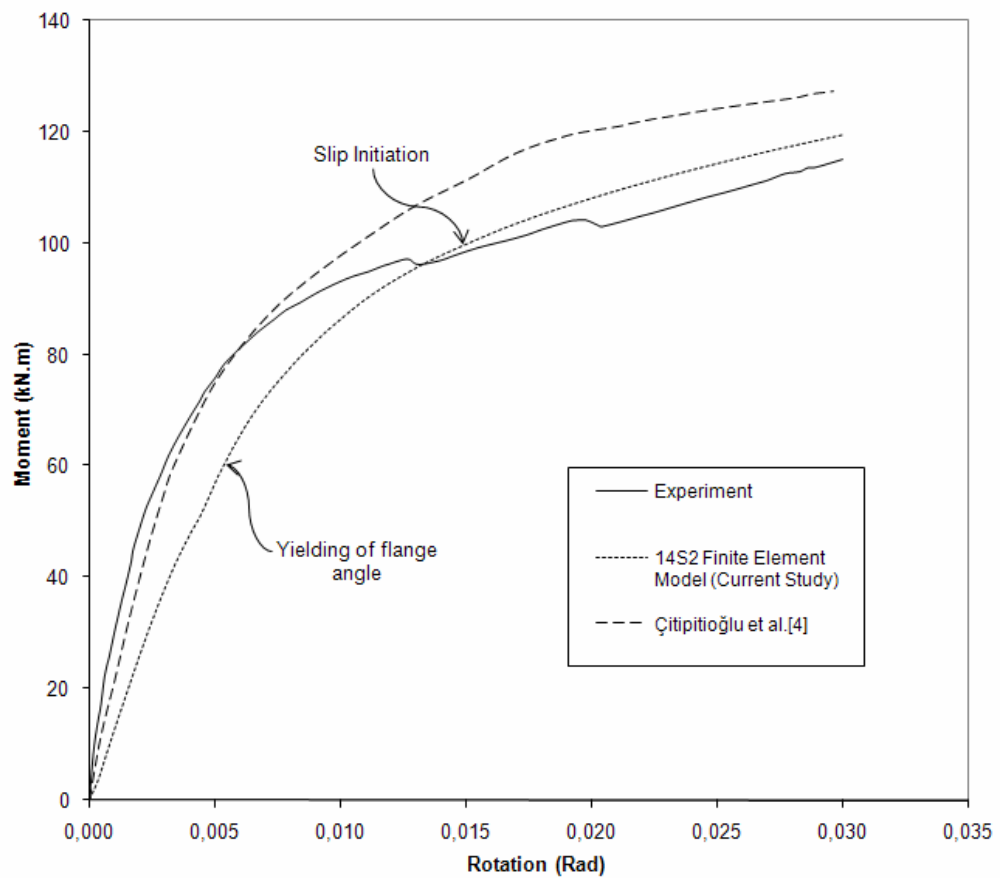


**Figure 2-9 Analysis Result and Comparison of the 14S2 Model**

The results obtained for 14S2 is similar to the ones in 14S1, where the same observations for both the initial and nonlinear/plastic stiffness are concluded. In Figure 2-9, the ultimate moment of 14S2 is 25% larger than that in Figure 2-7 for 14S1 since 14S2 specimen has thicker flange angles, and this increase is well predicted by the current study. Figure 2-9 also shows where the yielding of flange-angle occurs and where the slip initiates. The marked points are taken out from the finite element simulation and are given only for 14S2 specimen in order to inform about the occurrence of these local actions in such connections.

An overall conclusion from 14S1 and 14S2 specimens are as follows: the ultimate moment capacity is basically irrelevant of the yield strength of steel defined in analysis. The nonlinear range of connection response is mainly affected by slip in the connection and in this regards the current study predicts the nonlinear range well. On the other hand, the connection simulation of current study could not quite catch the initial stiffness of the experimental result. The most probable reason of this error is due to the difference in the used materials for the flange angles. The given yield strength value by Azizinamini [11] for flange angle material is observed to be out of range for being A36 steel as presented in Table 2-3. When the presented yield strength by Azizinamini is used in the current analysis, an increase in initial stiffness is observed, yet this however results in an overestimation of nonlinear response. Thus the current study followed the suggested yield strength values for steel from design codes.

Specimen 14S3 of Azizinamini is different than the other 14Sx specimens due to its web angles' properties as stated in Table 2-1. This specimen consists of W14x38 (W360x57) beam, L6x4x3/8 (L152x102x9.5 mm) top and seat angle, L4x3<sup>1/2</sup>x1/4 (L102x89x3.6 mm) web angles, which has 2 bolts instead of 3 and smaller in length, with 3/4 in (19.1 mm) bolts. This model is very similar the 14S1 model where only the length of web angles and the amount of bolts attached to it are changed. The results of the experimental data and numerical simulation are presented in Figure 2-10.

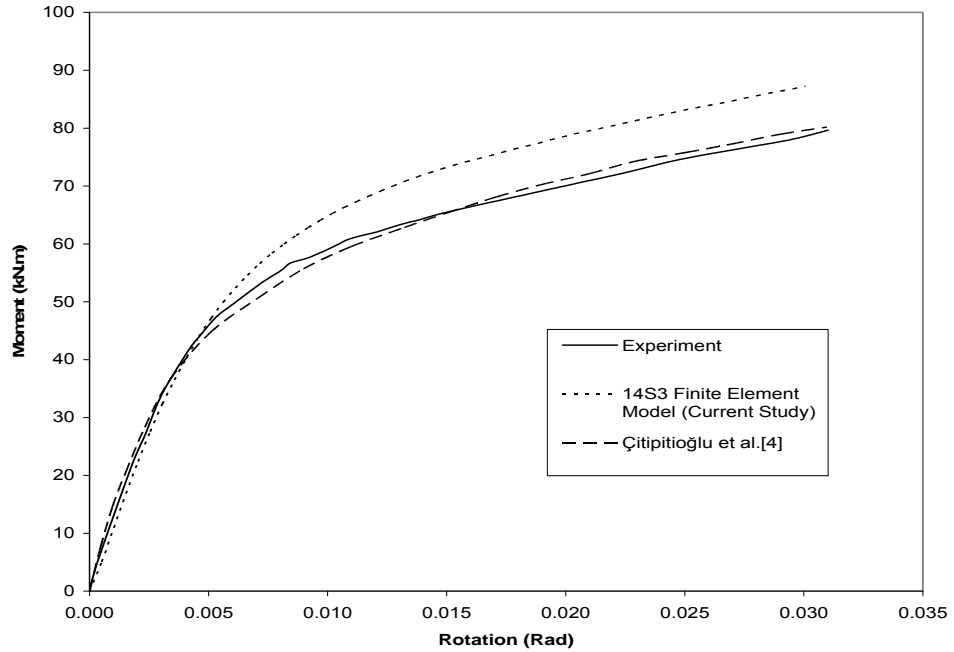


**Figure 2-10 Analysis Result and Comparison of the 14S3 Model**

Figure 2-10 illustrates a reversal of the trend of the current study observed in 14S1 and 14S2 specimens. The analysis for 14S3 captures the initial stiffness of the connection better than the previous simulations. The stiffness of the nonlinear part of the connection is caught better with 6% drift from the nonlinear part which can be seen as an acceptable result in such analysis. The reversal in trend is thought to be due to the use of smaller length for web angle for this specimen.

Another model simulated within the current study from Azizinamini experiments is specimen 14S4. This specimen is similar to 14S1 where the thickness of the web angles is different between the two. 14S3 consists of W14x38 (W360x57) beam, L6x4x3/8 (L152x102x9.5 mm) top and seat angle, L4x3<sup>1/2</sup>x3/8 (L102x89x9.5 mm) web angles with 3/4 in (19.1 mm) bolts. In the simulation, a pretension force equal to 28 kip (124 kN) and friction coefficient  $\mu=0.35$  are employed. The result of the analysis by current study is presented in Figure 2-11, where the experimental result and the result of Citipitoglu et.al [4] are also provided.

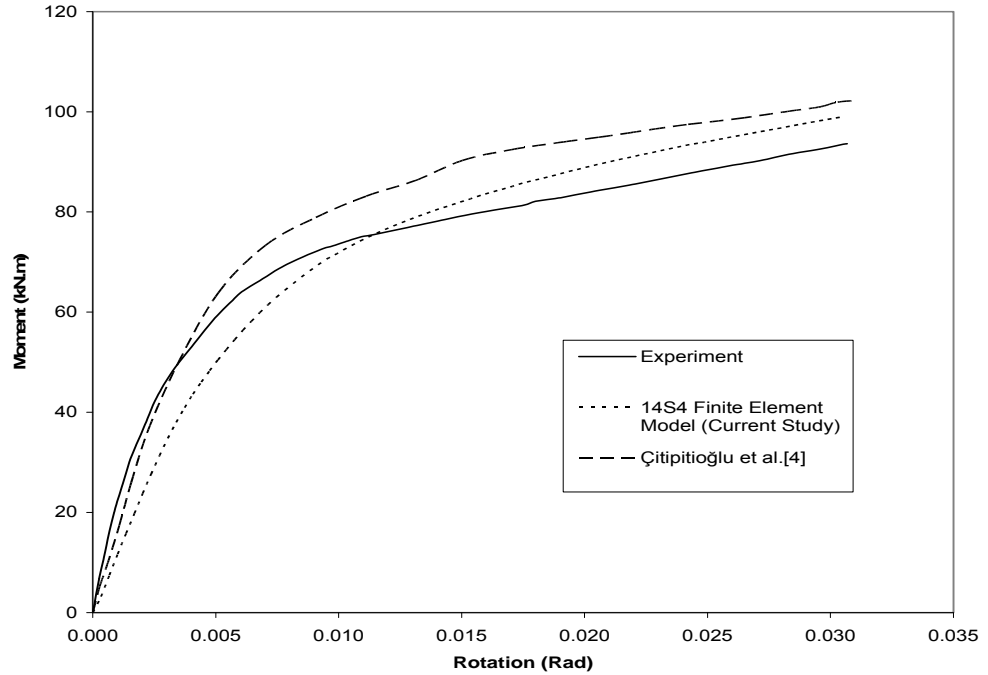


**Figure 2-11 Analysis Result and Comparison of the 14S4 Model**

The moment-rotation response obtained from the finite element analysis of 14S4 with current study is again back on track with the trend observed in the results obtained for 14S1 and 14S2 specimens. In Figure 2-11, the initial stiffness of the connection is estimated lower than the experimental one, and the nonlinear response is estimated well contrary to the result obtained in model 14S3. The stiffness of the nonlinear part also fitted well which seems to be the characteristic feature of the current study.

The flange and web angle thickness values of specimens 14S1 to 14S4 by Azizinamini are all different, and from these specimens we conclude that a change in the web angle thickness is observed to have an insignificant effect on the moment capacity of a connection. On the other hand, variation in flange angle thickness changes the moment capacity significantly. The current finite element study has accurately captured this physical reality observed in the experimental tests as presented in Figures 2-7 to 2-11.



The last connection specimen that is simulated for top and seat angles with double web angles connection is the Azizinamini's 14S5 specimen. This connection differs from other 14Sx specimens with respect to the bolt diameter. The connection test setup consists of the following components: W14x38 (W360x57) beam, L6x4x3/8 (L152x102x9.5 mm) top and seat angle, L4x3<sup>1/2</sup>x1/4 (L102x89x3.6 mm) web angles with 7/8 in (22.3 mm) bolts. Since the bolt diameter changed, the pretension value is raised from 28 kip (124 kN) to 39 kip (173kN). The value of friction coefficient is not changed and taken as  $\mu=0.35$ . The output of the finite element study and experimental data are presented in Figure 2-12.

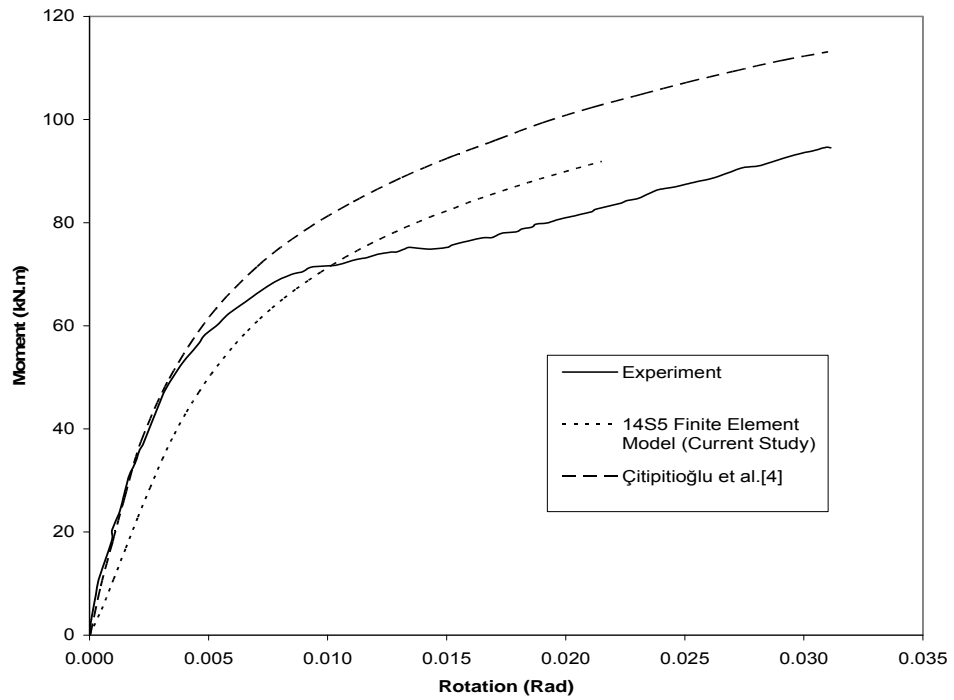


**Figure 2-12 Analysis Result and Comparison of the 14S5 Model**

The last simulation model also shows a lower initial stiffness and again a more accurate nonlinear stiffness. As seen from the nonlinear part, the corresponding ultimate moment obtained from current analysis is also very close to the ultimate moment of the test. The distinct character of the 14S5 model is that the stress level in the bolts exceeds the ultimate stress of the ASTM A325 bolts before the rotation reached 0.03 radians. The simulation model in this respect could not handle the large deformation with the attained stress levels and could not converge to a solution in this highly nonlinear part of the analysis. The amount of plastic deformation in the bolts is thought to be the main reason in not reaching a converged solution with desirable displacements. In this perspective, the stress levels in the flange and web angles go beyond yield values, whereas the stress levels in the angles do not reach ultimate values when failure occurs in the bolts in finite element simulation.

The analyzed five specimens 14S1 to 14S5 from Azizinamini's experimental work show that the top and seat angles with double web angles connections can be effectively modeled through finite elements simulations. It is seen that the finite element study by Citipitioglu et.al [4] approximates the initial stiffness more closely than the current study for the top and seat angle with double web angle connections. In general, the slope in the nonlinear range from current study matches the experimental curves more closely than that obtained in Citipitioglu's study. Despite this fact, Citipitioglu's analyses on some other specimens of Azizinamini have yielded about 45% error in the initial stiffness (14S8) with much greater errors in ultimate moments.

It can be concluded that a perfect one to one match with experimental curves is difficult due to several uncertainties and assumptions related to both the experimental tests and the finite element modeling of such complex nonlinear problems. However, a relatively close match is sufficient enough to draw conclusions about connection response, and the current study is able to attain this. Furthermore, the main characteristics of a top and seat angle with double web angles connection behavior are accurately captured within the approach followed in this thesis.

#### ***2.4.2 The Results of Top and Seat Angle Connection without Double Web Angles***

The top and seat angle connection is the other type of semi-rigid connection that is modeled in this thesis. The top and seat connection has got a moment capacity less than top and seat angle connection reinforced with double web angles. Nevertheless, the connection moment capacity is great enough to place it in the category of semi-rigid connection.

There is a lack of experimental analysis for top and seat angle connection and many of conducted experimental researches do not provide enough information to simulate connection correctly. In this respect, the researches are either too old to gather required data or lack of information to cover the basic aspect of the simulations.

As discussed in Section 2.2, the specimens for the top and seat angle connection are selected from a recent experimental study of Kukreti et al. [13], where the specimens were tested under cyclic loading conditions. The envelope of the moment-rotation response from experimental data is considered for comparison of the current finite element study. The test specimens and the general setup of the test configuration were explained in Section 2.2.

Two of the test specimens of Kukreti et.al are considered for finite element analysis. The first model investigated is Test 5 which has got the properties of L6x4x3/4 (152x102x19 mm) flange angles and 3/4 in (19.1 mm) bolts. In the experimental study, the bolts were tightened to develop a pretension force equal to their proof load; thus the pretension value in the current finite element study is chosen as 28 kip( 124 kN) and the value of friction coefficient is taken as equal to 0.35 ( $\mu=0.35$ ) in the case of Class A faying surfaces.

The deformed shape of the simulation model and the corresponding envelope of the moment rotation curve from experiment are presented in Figures 2-13. and 2-14, respectively.

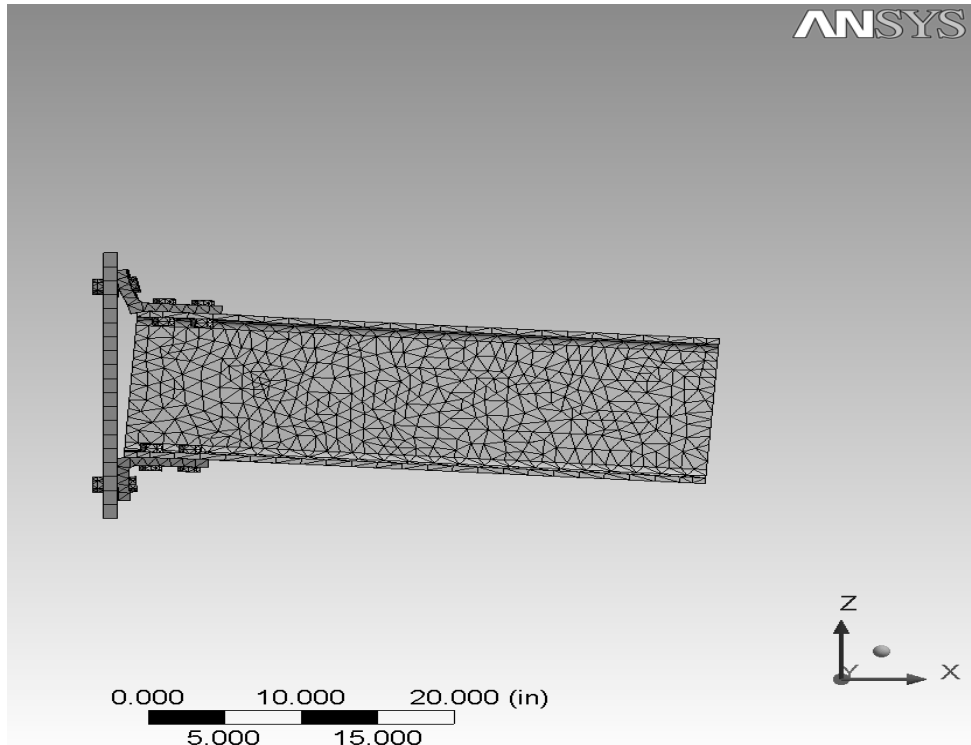


**Figure 2-13 A Sample Deformed Shape of TS Connections**

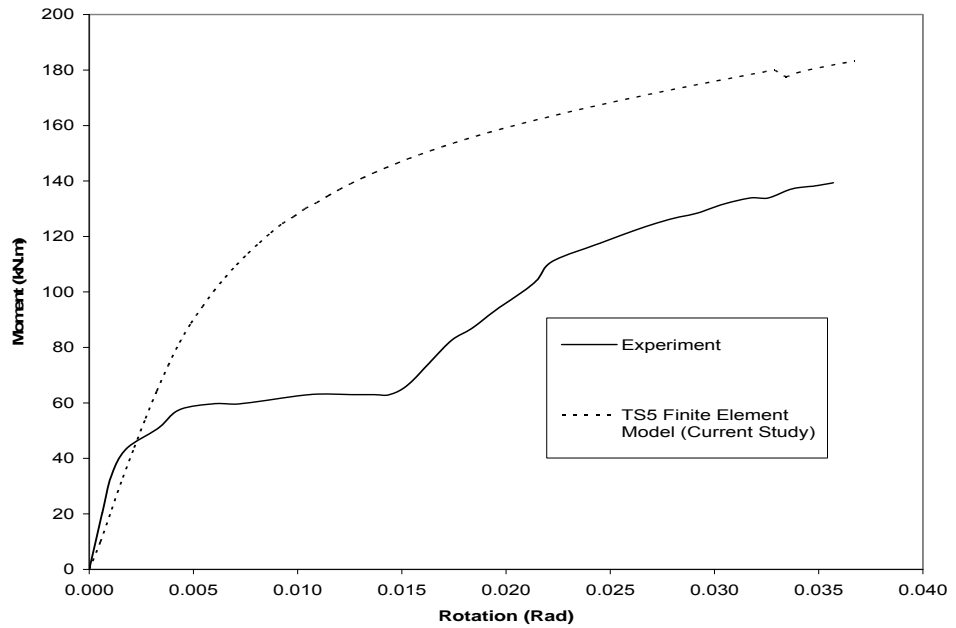


**Figure 2-14 Comparison of the Test and Finite Element Analysis of TS5 Connection**

In the experimental analysis, the TS5 connection has shown a deformation pattern that can be investigated within three regions. In the first region, deformation pattern is linear. Just after the initial stage, there is a part where great amount of deformation occurs without any significant moment gaining. This process is followed with the hardening stage just after the second stage. In this part, increase in the moment capacity is significant and the stiffness is close to the initial value. Then, the stiffness decreases, and the gain in moment capacity reduces.

On the other hand, the simulation conducted within the concept of this thesis work shows a smoother response than that observed in the experiment. The initial stiffness and the stiffness in the last nonlinear part of the experimental curve are captured closely, yet there is a big drift between the results of ultimate moment. The overall differences in the response are basically caused due to the monotonic nature of analysis conducted in the current study, while the response plotted in Figure 2-14 is extracted from cyclic loading. The second stage of the experimental curve, where significant rotation occurs without any moment increase, is not predicted. This most probably occurs due to the enormous amount of slip where the reason lies in test environment. The regaining of the initial stiffness after this amount of deformation also shows the fact that this region has to be reconsidered. The ultimate moment capacity from the current finite element study is overestimated in the order of 25%. The reason of the difference between the ultimate moments obtained from the experiment and the analysis is thought to be due to the premature slip between the steel parts. It is also believed that the thickness of flanges plays a role in this highly nonlinear response of these types of connections. The next specimen by Kukreti et.al has a thinner flange thickness than this one, and a better match is observed for that specimen.

The other simulation analysis conducted within the top and seat angle connections analyses is TS6 specimen tested by Kukreti et al.[13]. The connection consists of L6x4x1/2 (152x102x12.7 mm) flange angles and 3/4 in (19.1 mm) bolts. This connection has a thinner flange angle than the TS5 specimen. Since the bolts diameters are not changed, the applied pretension value is remained as 28 kip (124 kN) and the friction coefficient is taken as  $\mu=0.35$ . The result of the finite element simulation and the experimental one is shown in Figure 2-15.

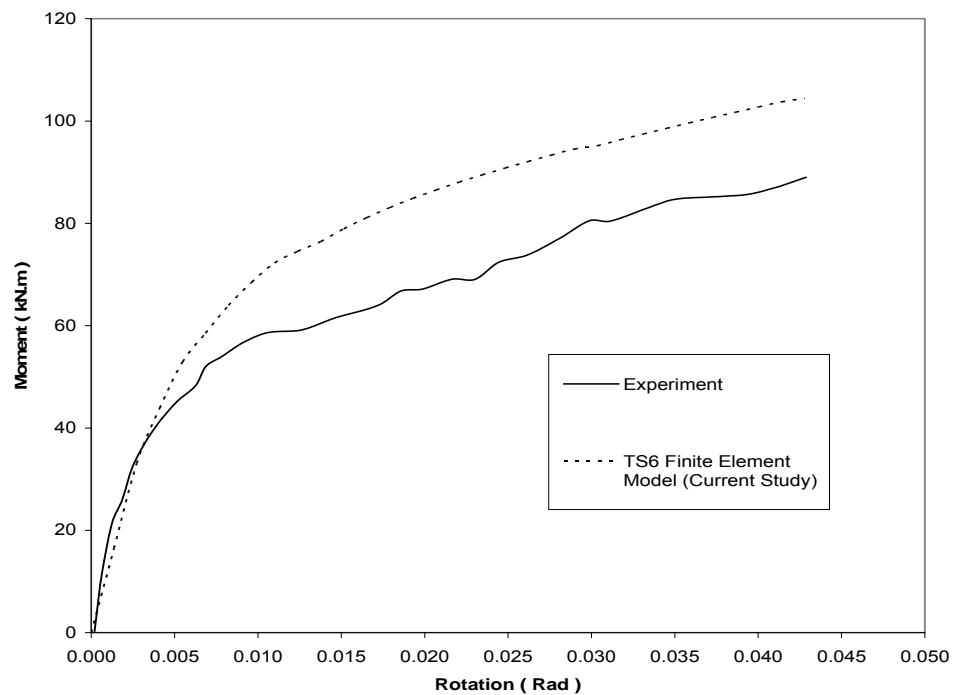


**Figure 2-15 Comparison of the Test and Finite Element Analysis of TS6 Connection**

Experimental curve of TS6 connection does not show a stage where a significant rotation occurs without any moment increase as observed in TS5 specimen. The path of the moment-rotation response of the connection obtained from the current study in Figure 2-15 is in complete accordance with the pattern of the experimental data. The initial stiffness of the connection and the stiffness of the nonlinear part are closely approximated. The error in the ultimate moments in Figure 2-15 is about 15%, and a closer match is attained than that in TS6 specimen.

The comparison of the responses between TS5 and TS6 specimens reveals the following: the experimental moment-rotation curve and the deformation pattern of specimen TS6 are more reliable than TS5. The current finite element study is not able to capture the complex response of TS5 specimen, where the rate of loading is caused to be the main reason behind the error. The finite element model did not capture the effect of the deterioration or pinching of the elementary parts. Furthermore, thicker flanges might have an influence in the complex response of TS5 with respect to TS6 specimen that has thinner flange. The effect of the flange thickness on the overall deformation pattern is more clearly seen when the moment rotation responses of the TS5 and TS6 are compared simultaneously.

In conclusion of the chapter, the analyzed models for top and seat angle connections (both with and without double web angles) are chosen to give an inside review of the moment and rotation capacities of the connections in consideration with different variables. The capabilities of the finite element model on such connections are represented with the comparison of results with experimental ones. The possible reasons between the differences of the results obtained from nonlinear finite element analysis and the experimental data are also discussed. The next chapter of the thesis will continue with the simplified mathematical models that are developed for these types of connections. 3-D finite element analysis can not compete with the performance of the moment-rotation relations suggested by these mathematical models, and the development and verification of such simplified expressions enable the implementation of semi-rigid connection behavior into the analysis of structural systems.

## **CHAPTER 3**

### **MATHEMATICAL MODELS FOR SEMI-RIGID CONNECTIONS**

The mathematical relations for steel beam to column connections were first proposed as early as 1930's when structural steel was initiated for use as indicated in Chapter 1. The first models were excessively simplified and were not that much accurate. Furthermore, the variation for each parameter was too wide to represent a good deal of combination for mathematical equations. To come up with better model proposals, a great amount of effort was spent in conducting physical tests by different researchers. In this perspective, each test with different physical parameters led to a result in establishing a mathematical model to represent growing number of specimen data; thus the models became more accurate than before. The current mathematical models that are available in the literature are quite advanced than the ones dating back 1930's. Nevertheless, the accuracy of the mathematical models is still in doubt especially for certain types of semi-rigid connections with few available experimental data.

Finite element analysis is a convenient tool for the purpose of cross checking the accuracy of mathematical models and finite element analysis, since the available test data can be used to check the validity of both. For this reason, finite element analysis will become a substitute for the expensive tests that would provide reliable data for a widening range of connection types and parameters. Different properties can be tested on the platform of finite element simulation; however, engineers in practice seek to use simple and accurate equations for the design of connections instead of going through a time consuming and relatively cumbersome 3-D finite element analysis of each connection. Furthermore, engineers also want to analyze the structural system as a whole, and this is usually performed with beam-column



elements but not with 3-D solid finite elements. Thus, it is important to establish simplified mathematical models in the form of moment-rotation relations. The question at this point is whether 3-D finite element analysis gives enough information to represent connection response so that researchers can avoid conducting expensive tests in deriving these simplified mathematical models.

In this chapter, the mathematical models proposed for the semi-rigid connections are presented and investigated, and the results of the finite element analysis conducted in Chapter 2 are compared with some of these mathematical models and a brief discussion is presented.

### **3.1 Review of the Mathematical Models and Definitions**

#### ***3.1.1 Linear Connection Model***

The simplest mathematical model that can be found in literature is the linear connection model. The model itself needs only one connection parameter which is the initial stiffness. The connection model was suggested by different researchers to be used in early stages of developing analysis methods for semi-rigid joints and in the bifurcation and vibration analysis of semi-rigid frames due to the simplicity of the model [27]. The model can be described as follows:

$$M=R_{ki}*\theta \tag{3.1}$$

in which  $R_{ki}$  stands for the initial stiffness of the connection which can be defined in terms of the beam stiffness. One of the suggestions for the initial stiffness of the connection was done by Lightfoot and LeMessurier [27, 28] as the following expression;

$$R_{ki} = \lambda \frac{4EI}{L} \tag{3.2}$$

where  $EI$  ,  $L$  stand for the beam bending rigidity and length, respectively, and  $\lambda$  is called as the rigidity index that varies from 0 to 1 accounting for pinned connection to fixed connection, respectively.

Another suggestion for the same model was done by Romstad and Subramanian [27, 29] by using a fixity factor instead of rigidity index as follows:

$$R_{ki} = \frac{\eta}{1-\eta} \left( \frac{4EI}{L} \right) \quad (3.3)$$

where the fixity factor  $\eta$  changes from 0 to 1 to represent ideally pin and fixed connections, respectively.

This model is the most simplified model available in literature and the value of the single parameter can be easily found from a simple elastic test of the connection. Nevertheless, this model fails when deformations exceed the linear range. This model is recommended and mostly used in vibration and bifurcation analyses [27].

### **3.1.2 Multi-linear Connection Model**

The multi-linear mathematical model was derived in order to obtain a better representation of the nonlinear behavior of connections when the linear range of response is exceeded. The most basic form of the multi-linear model is bilinear model, which is suggested by different researchers from 1960's to current time [13, 27].

The multi-linear model parameters change from researcher to researcher. One typical example for a multi-linear model was presented by Kukreti et al. [13], where a bilinear curve was adopted to represent the overall behavior of the top and seat angle connections. The parameters in that research were obtained from the experimental data by curve fitting.

Although the multi-linear models perform better than the linear ones, discontinuities in slope sometimes lead to divergence and complexities in numerical analysis, thus the development of smoother functions for moment-rotation relations became desirable.

### 3.1.3 Polynomial (Frye and Morris) Model

The polynomial model is one of the most widely known mathematical models for connections, and it is adopted by many researchers due to its simplicity. The procedure of polynomial model was extensively used in steel beam to column connections for the first time by Frye and Morris [5, 17, 27, 30]; however, it was actually formulated before by Sommer [5, 17, 27, 31]. Despite this fact, the model is called as Frye and Morris polynomial model in literature, and the formulation is expressed as follows:

$$\phi = C_1(KM)^1 + C_2(KM)^3 + C_3(KM)^5 \quad (3.4)$$

where  $K$  is the standardization parameter that depends on geometrical properties and connection type.  $C_1$ ,  $C_2$  and  $C_3$  values are the curve fitting constants obtained from the experimental data.

The stiffness than can be calculated as the first derivative of the moment rotation function as follows:

$$R_k = \frac{\partial M}{\partial \phi} = \frac{1}{C_1 K + 3C_2 K(KM)^2 + 5C_3 K(KM)^4} \quad (3.5)$$

and the initial stiffness that is the stiffness where the moment is equal to zero is calculated as;

$$R_{ki} = \left. \frac{\partial M}{\partial \phi} \right|_{M=0} = \frac{1}{C_1 K} \quad (3.6)$$

The parameters required for the Frye and Morris polynomial model can be found in Table 3.1, and the definitions of the geometric properties listed in the table for top and seat angle connections (with or without double web angles) can be found in Figure 3.1 [5, 27, 30].

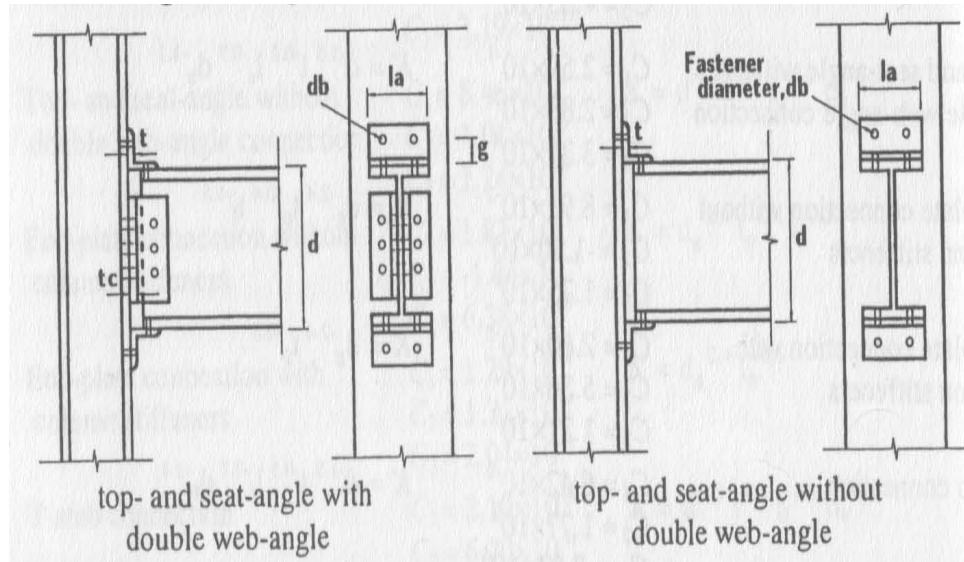


**Figure 3-1 Size Parameters for the Top and Seat Angle Connections of the Frye and Morris Polynomial Model [5]**

**Table 3-1 Standardization Constants for Frye and Morris Polynomial Model (All Size Parameters are in cm) [5]**

Connection types	Curve-fitting constants	Standardization constants
Single web-angle connection	$C_1 = 1.67 \times 10^0$ $C_2 = 8.56 \times 10^{-2}$ $C_3 = 1.35 \times 10^{-3}$	$K = d_a^{-2.4} t_a^{-1.81} g^{0.15}$
Double web-angle connection	$C_1 = 1.43 \times 10^{-1}$ $C_2 = 6.79 \times 10^1$ $C_3 = 4.09 \times 10^5$	$K = d_a^{-2.4} t_a^{-1.81} g^{0.15}$
Top- and seat-angle with double web-angle connection	$C_1 = 1.50 \times 10^{-3}$ $C_2 = 5.60 \times 10^{-3}$ $C_3 = 4.35 \times 10^{-3}$	$K = d^{-1.287} t^{-1.128} t_c^{-0.415} l_a^{-0.694} (g-d_b/2)^{1.350}$
Top- and seat-angle without double web-angle connection	$C_1 = 2.59 \times 10^{-1}$ $C_2 = 2.88 \times 10^3$ $C_3 = 3.31 \times 10^4$	$K = d^{-1.5} t^{-0.5} l_a^{-0.7} d_b^{-1.1}$
End-plate connection without column stiffeners	$C_1 = 8.91 \times 10^{-1}$ $C_2 = -1.20 \times 10^4$ $C_3 = 1.75 \times 10^8$	$K = d_g^{-2.4} t_p^{-0.4} t_f^{-1.5}$
End-plate connection with column stiffeners	$C_1 = 2.60 \times 10^{-1}$ $C_2 = 5.36 \times 10^2$ $C_3 = 1.31 \times 10^7$	$K = d_g^{-2.4} t_p^{-0.6}$
T-stub connection	$C_1 = 6.42 \times 10^{-2}$ $C_2 = 1.77 \times 10^2$ $C_3 = -2.03 \times 10^4$	$K = d^{-1.5} t^{-0.5} l_t^{-0.7} d_b^{-1.1}$
Header-plate connection	$C_1 = 6.14 \times 10^{-3}$ $C_2 = 1.08 \times 10^{-3}$ $C_3 = 6.05 \times 10^{-3}$	$K = t_p^{-1.6} g^{1.6} d_p^{-2.3} t_w^{-0.5}$

The procedure of the development of the model was pursued by Picard et al. [32], Altman et al. [33] and Goverdhan [34] for different types of connections [5].

Although the Frye and Morris polynomial model has certain advantages in structural analysis due to its simplicity, there are certain pitfalls due to the nature of polynomial. The utilized polynomial function could yield negative first derivatives in certain ranges of connection parameters, i.e. negative tangent stiffness for Equation 3.5, and this leads to a certain difficulty in the structural analysis when the polynomial model is used [5].

### ***3.1.4 The Power Model***

The power model has been developed and improved by various researchers. The very first power model was composed of two parameters and suggested by Batho et al. [34] and Krishnamurthy et al. [35]. The following form of equation was suggested for the two parameter power model:

$$\phi = aM^b \quad (3.7)$$

in which a and b are the curve fitting parameters. This model, as seen from the parameters, requires great amount of sampling from experimental researches of connection types and therefore it is not quite appropriate for the structural analysis.

On the other hand, the three parameter power model by Colson and Louveau [36] and Attiogbe and Morris [39] is found suitable and rational for the representation of connection behavior. These three-parameter models are based on the elastoplastic stress-strain model proposed previously by Richard [37] and later applied to nonlinear structural analysis by Goldberg and Richard [38].

Using the initial connection stiffness  $R_{ki}$  and the ultimate moment capacity  $M_u$  of the connection, the three-parameter power model represents the moment-rotation (M-  $\theta$ ) relationship as follows:

$$M = \frac{R_i \phi}{\left[ 1 + \left( \frac{\phi}{\phi_0} \right)^n \right]^{1/n}} + R_{kp} \phi \quad (3.8)$$

in which  $R_{kp}$  = plastic connection stiffness;  $R_i = R_{ki} - R_{kp}$ ;  $\phi_0$  = a reference plastic rotation; and  $n$  = shape parameter.

Assuming moment-rotation curve flatten out near the state of ultimate strength of connection, the plastic connection stiffness becomes zero. Thus, the three parameter power model reduces to the following form:

$$M = \frac{R_{ki} \phi}{\left[ 1 + \left( \frac{\phi}{\phi_0} \right)^n \right]^{1/n}} \quad (3.9)$$

in which  $\phi_0 = M_u / R_{ki}$ .

The shape parameter ( $n$ ) can be determined by using the method of least squares for the differences between the predicted moments and the experimental test data. The other parameters,  $R_{ki}$  and  $M_u$  respectively, can be found as suggested by Kishi and Chen [40].

For the initial stiffness  $R_{ki}$ , the following assumptions are made [41]:

- The center of rotation for the connection is located at the leg adjacent to the compression-beam flange at the end of the beam (point C in Figure 3-2).
- The angle leg connected to column behaves linear elastically, and the adjacent leg connected to the beam undergoes rigid body motion.
- The vertical leg of the top angle is given along the line of the nuts edge for bolted fasteners (Figure 3-3).
- The web angle is deformed in such a way that it is similar to the top angle part (Figure 3-4).

- The bearing-pressure is distributed uniformly along the outstanding leg of the seat angle (Figure 3-5).

Then utilizing simple elastic beam theory with these assumptions and considering shear deformation, the contribution of each part of the connection to initial stiffness can be written as follows:

$$R_{kit} = \frac{3EI_t(d_1)^2}{g_1(g_1^2 + 0.78t_t^2)} \quad (3.10)$$

$$R_{kis} = \frac{4EI_s}{l_{s0}} \quad (3.11)$$

$$R_{kia} = \frac{6EI_a(d_3)^2}{g_3(g_3^2 + 0.78t_a^2)} \quad (3.12)$$

where  $R_{kit}$ ,  $R_{kis}$  and  $R_{kia}$  stand for the initial stiffness contribution of top angle, seat angle and web angles, respectively.  $EI_t$ ,  $EI_s$ ,  $EI_a$ , stand for the bending rigidities of the top, seat and web angles. The other properties are all geometrical and are shown in Figures 3-2 to 3-5.

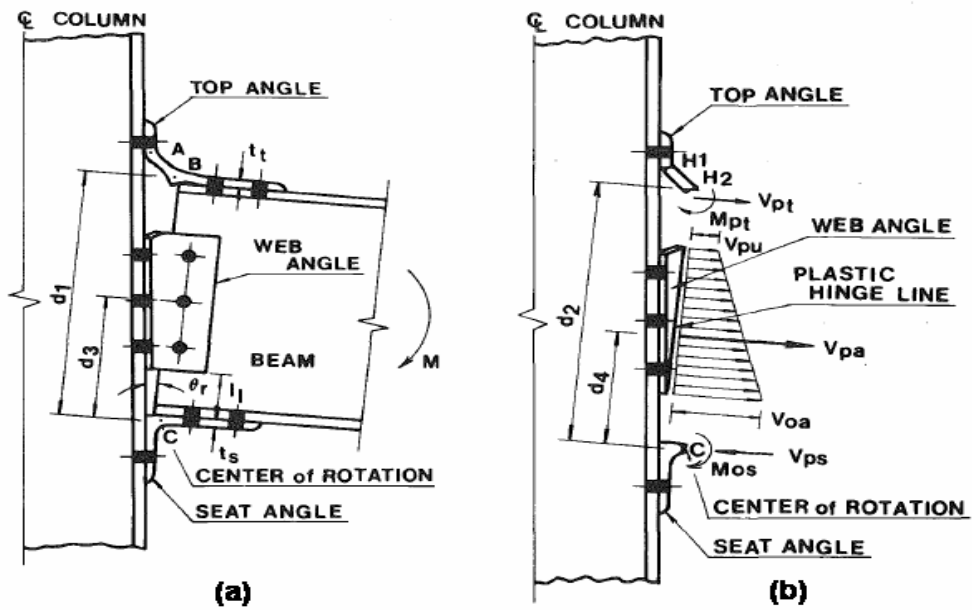


Figure 3-2 a) Deflection Configuration of Elastic Condition of the Connection, b) Applied Forces in Ultimate State of the Connection [40]

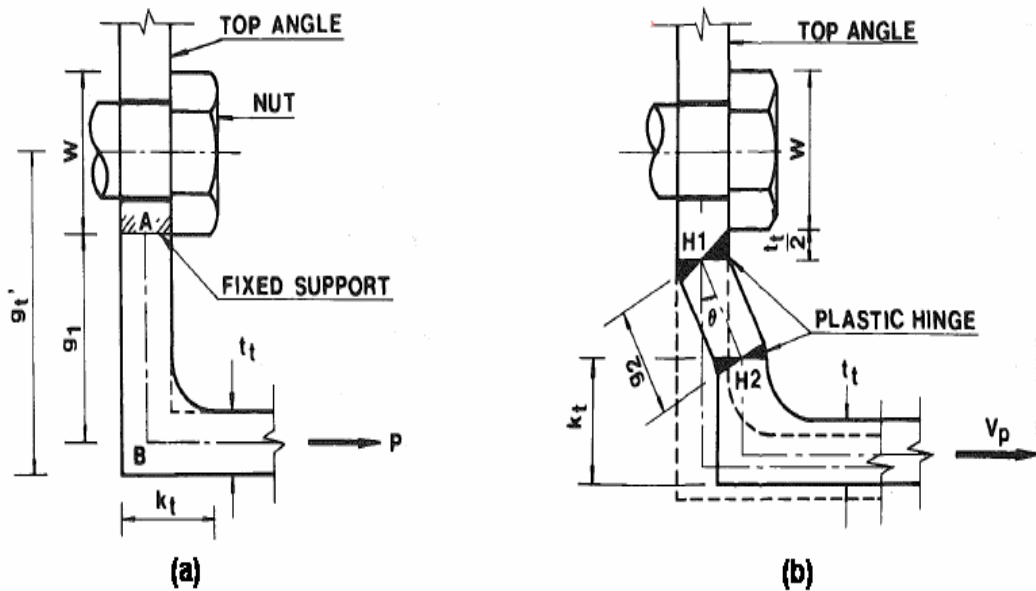


Figure 3-3 Top Angle Connection a) Cantilever Beam Model of Ultimate Condition b) Mechanism of Top Angle at Ultimate Conditions [40]



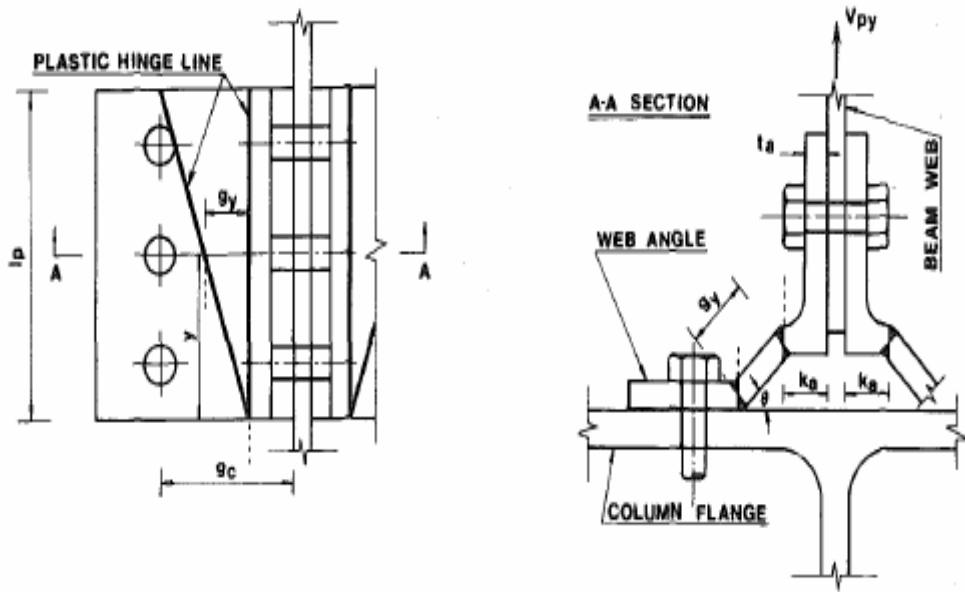


Figure 3-4 Mechanism of Web Angle Connection at Ultimate State [40]

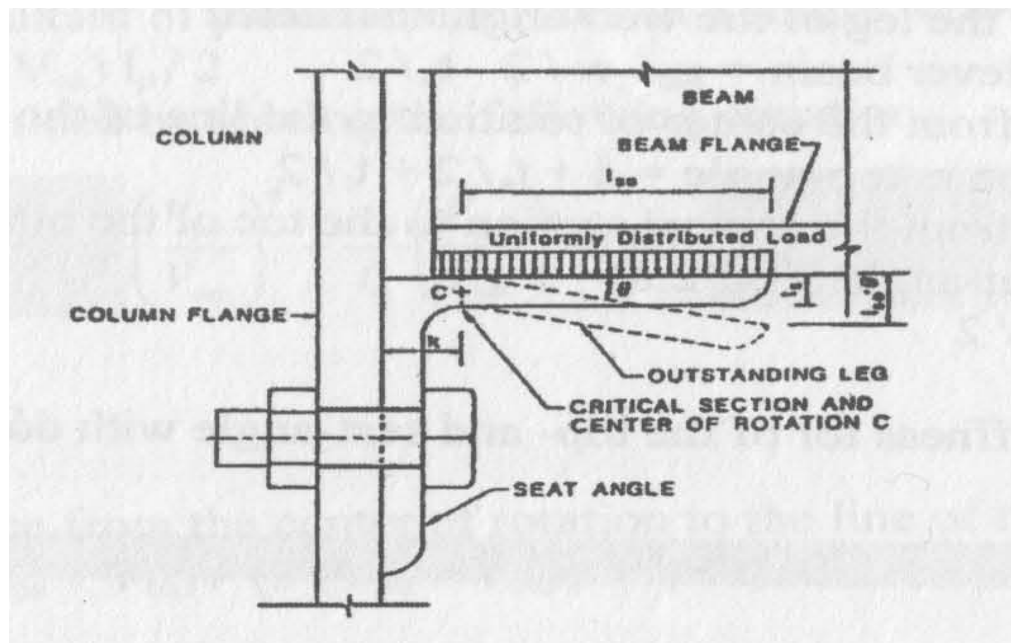


Figure 3-5 Seat Angle Connection [5, 41]

The overall initial stiffness is simply the sum of the three contributions in Equations 3-10 to 3-12 and can be written as follows:

$$R_{ki} = R_{kit} + R_{kis} + R_{kia} \quad (3.13).$$

On the other hand, the ultimate moment capacity of the connection is very much dependent on the elastic-plastic collapse mechanism. In the model suggested by Kishi et al. [41], the collapse mechanism may be obtained by the summation of the plastic moment capacities contributed by each angle. In this perspective, plastic beam theory considering moment-shear interaction is used to evaluate ultimate moment capacity. This model uses Drucker's yield criterion [41] for moment-shear interaction. The application of the model to the top and seat angle connections gives the following ultimate moment value:

$$M_u = M_{os} + M_{pt} + V_{pt}d_2 + 2V_{pa}d_4 \quad (3.14).$$

in which  $M_{pt} = V_{pt}g_2/2$  is the plastic moment in the top angle;  $M_{os} = \sigma_y l_s (t_s)^2 / 4$  is the plastic moment in the seat angle;  $V_{pt}$  is the plastic shear force in the vertical leg of the top angle, which is found by solving the following equation;

$$\left(\frac{V_{pt}}{V_{ot}}\right)^4 + \frac{g_2}{t_t} \left(\frac{V_{pt}}{V_{ot}}\right) - 1 = 0 \quad (3.15).$$

where  $V_{ot} = \sigma_y l_s t_s / 2$ ;  $V_{pa} = (V_{pu} + V_{oa})l_p / 2$  is the resultant of plastic shear force in a single web angle;  $V_{pu}$  can be found by solving the following equation;

$$\left(\frac{V_{pu}}{V_{oa}}\right)^4 + \frac{g_y}{t_a} \left(\frac{V_{pu}}{V_{oa}}\right) - 1 = 0 \quad (3.16).$$

and finally  $V_{oa} = \sigma_y t_a / 2$ .

The definition of other geometric parameters is presented in Figures 3-2 to 3-5.

The last parameter that defines the three parameter power model is the shape parameter  $n$ , where the other parameters  $R_{ki}$  and  $M_u$  are defined above. The value of the shape parameter is determined from the experimental data by carrying out least mean square technique. The values for the top and seat angle connection are stated below as functions of  $\phi_0$ :

$$\begin{aligned} n &= 1.398 \log_{10} \phi_0 + 4.631; & \text{if } \log_{10} \phi_0 > -2.721 \\ n &= 0.827; & \text{otherwise} \end{aligned} \quad (3.17)$$

for the top and seat angle connection with double web angles;

$$\begin{aligned} n &= 2.003 \log_{10} \phi_0 + 6.070; & \text{if } \log_{10} \phi_0 > -2.880 \\ n &= 0.302; & \text{otherwise} \end{aligned} \quad (3.18)$$

for the top and seat angle connection without double web angles.

With the definition of the last parameter, the power model is completed with the formulation by Kishi et al. [41]. The model is an effective tool for structural analysis since Equation 3.9 gives direct and quick results for a desired point of the moment rotation curve.

The model is also adopted with slight differences to the Eurocode 3 [42], and it is recently used in a model by Faella et al. [17]. It is stated that Eurocode 3 [42] definition is a lower bound for this kind of connection response and the Kishi et al. [41] model is the upper bound solution. The model by Faella et al. [17] gives results in between these two power models. For completeness, these three models are revisited below.

In Eurocode 3 model, the equivalent T-stub is defined according to the following equations;

$$m_{ta} = l_t - t_t - e_t - 0.8r_t \quad \text{for } g \leq 0.4t_t \quad (3.19)$$

$$m_{ta} = l_t - 0.5t_t - e_t \quad \text{for } g > 0.4t_t \quad (3.20)$$

where the parameters in above equations are defined in Figure 3-6.

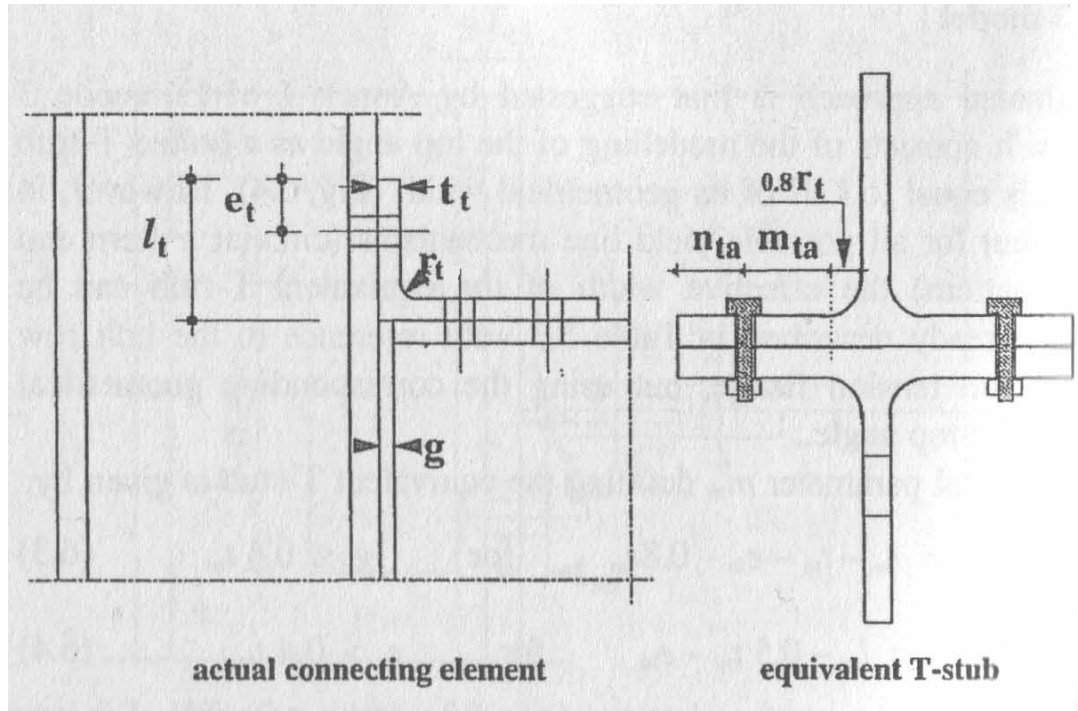


**Figure 3-6 The Geometrical Parameters of Eurocode 3 Model [17]**

The parameter  $m_{ta}$  is actually another definition for the distance for the location of plastic hinges of the top angle at ultimate state ( $g_2$  in Kishi et al. model). By considering Kishi et al. [41] and Eurocode 3 [42] model, Faella et al. [17] suggested another parameter to come up with a better solution for the distance in between plastic hinges. The parameter,  $\Psi$ , is defined as follows:

$$0 \leq \psi = 1.89 - 3.22 \left( \frac{t_t}{d_b \sqrt{g_2 / d_b}} \right) \leq 1 \quad (3.21)$$

where  $d_b$  is bolt diameter and the other parameters are as shown in Figure 3-3.

Then the parameter,  $\Psi$ , is further related with the following equation as;

$$m_{ta}^* = m_{ta} - \Psi \left( \frac{w}{2} + \frac{t_t}{2} + 0.2r_t \right) \quad (3.22)$$

In this equation,  $\Psi$  has a range of value in between 0 and 1, where 0 represents the Eurocode 3 definition and a lower bound solution, whereas 1 represents Kishi et al. model and an upper bound solution.

### 3.2 Comparison of Mathematical Models with Finite Element Analysis

In this thesis, the finite element analysis of top and seat angle connection with or without double web angles is pursued. The presented analyses in Chapter 2 were compared with experimental results and other finite element analysis results. This effort will now be complemented with comparison of the moment-rotation responses obtained in Chapter 2 with the mathematical models presented in Section 3.1. These simplified mathematical models actually form the basis of code equations used in practice.

The models which are compared in this part are the polynomial model [30], Kishi et al. model [41], Eurocode 3 model [17] and Faella et al. model [17]. The linear and the multi-linear models are skipped, since there is not enough information and sampling data about the conducted semi-rigid connection types. In Figures 3-7 to 3-13, the comparison of the experimental and finite element analysis results with these mathematical models are presented for the connections of 14S1 through 14S5 top and seat angle connection with double web angles of Azizinamini [11] tests and TS5 and TS6 top and seat angle connections tests of Kukreti et al. [13]. After the presentation of the results, brief discussion is provided.

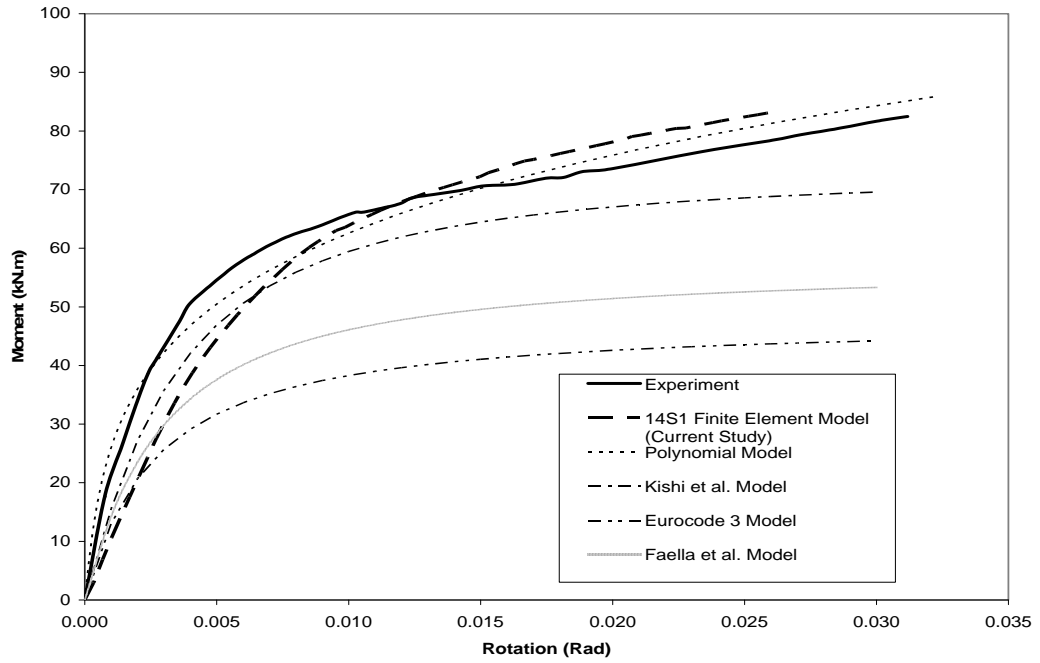


**Figure 3-7 Comparison of 14S1 Specimen**

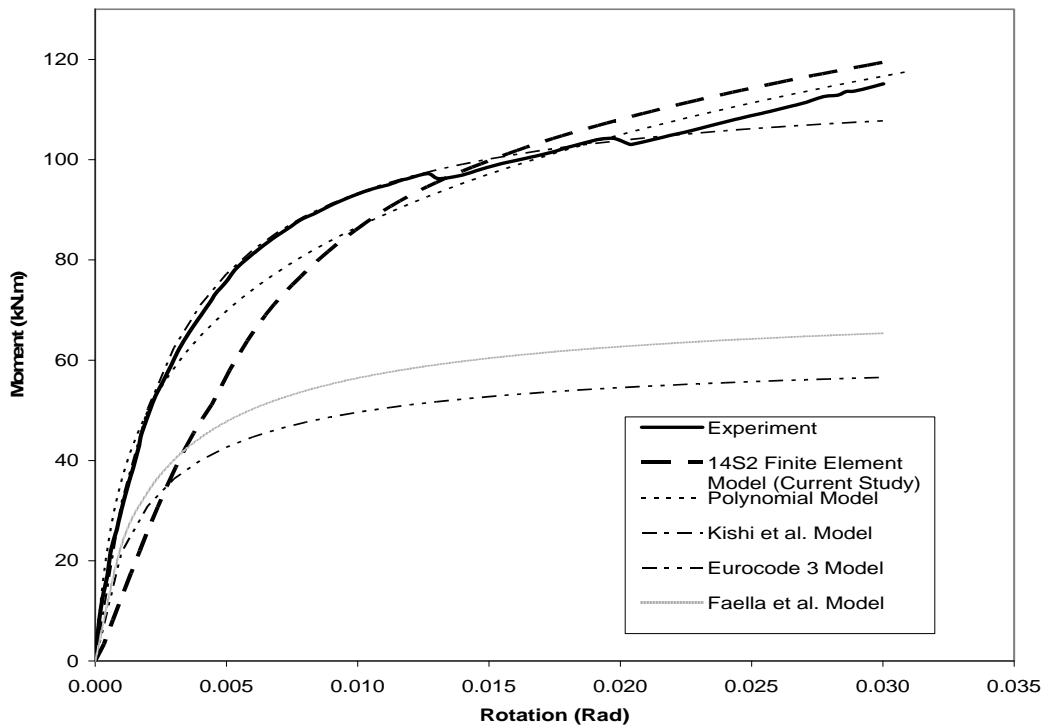


**Figure 3-8 Comparison of 14S2 Specimen**

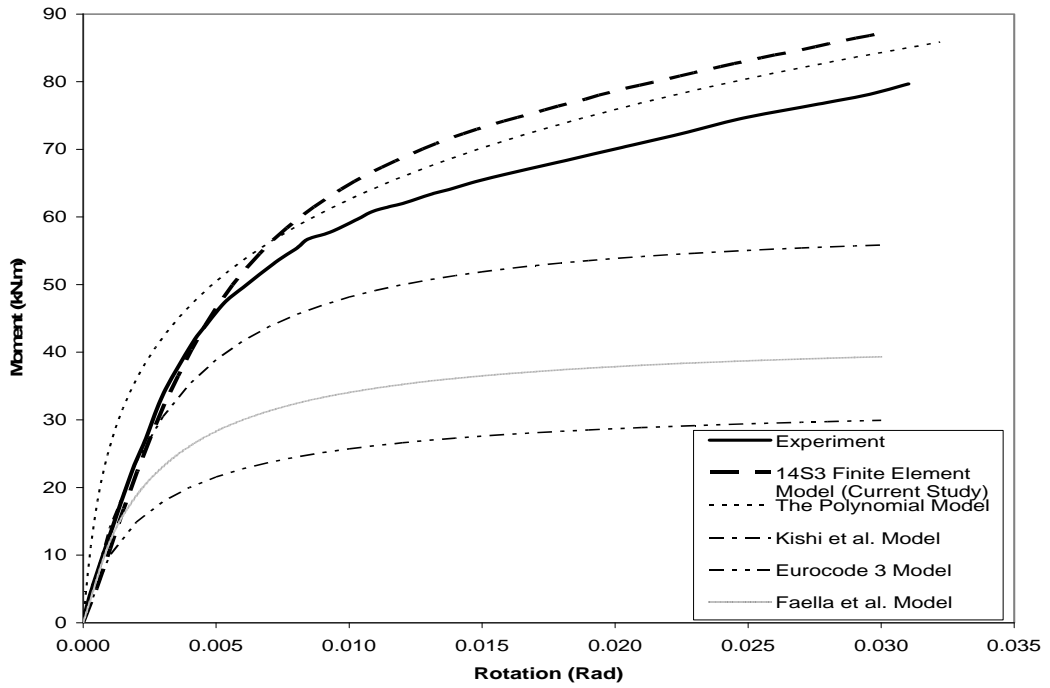


**Figure 3-9 Comparison of 14S3 Specimen**

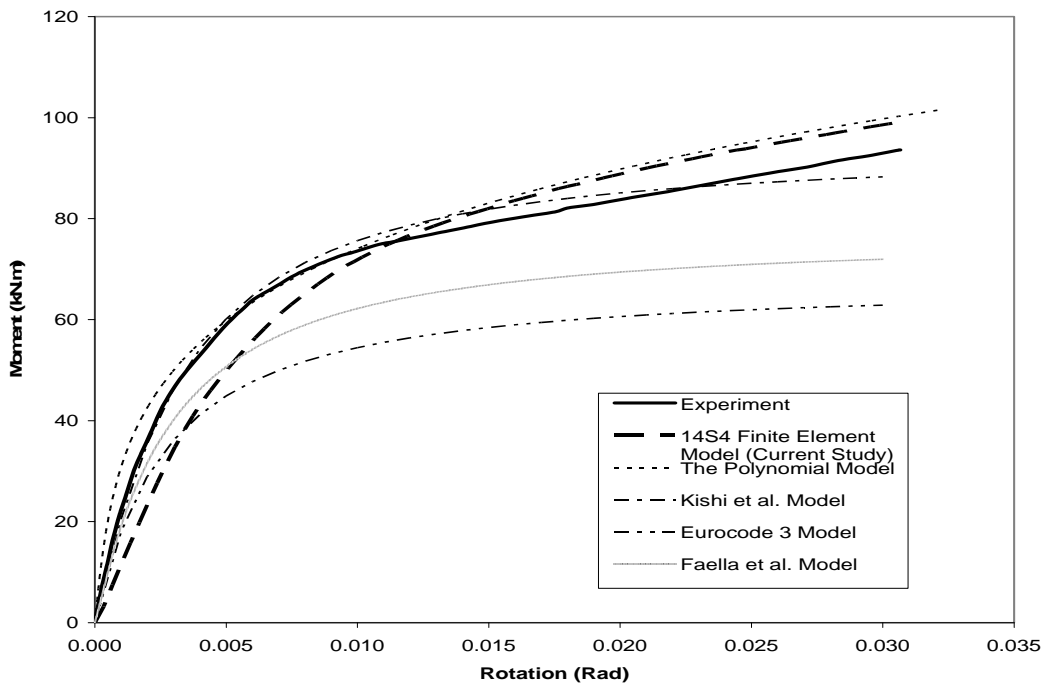


**Figure 3-10 Comparison of 14S4 Specimen**

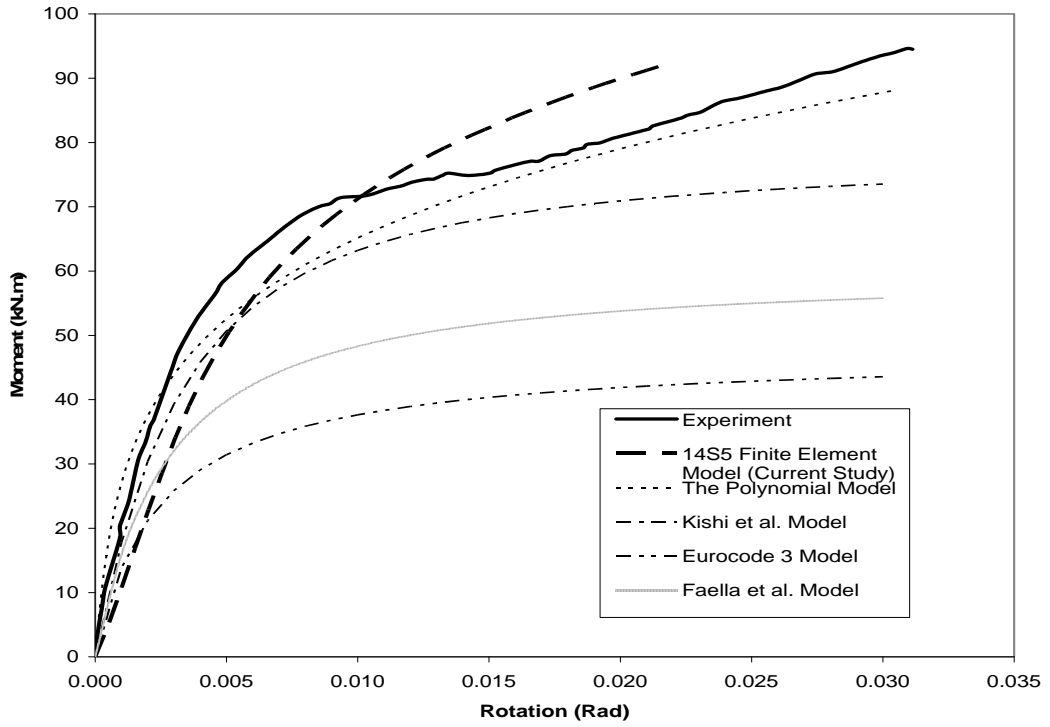


**Figure 3-11 Comparison of 14S5 Specimen**

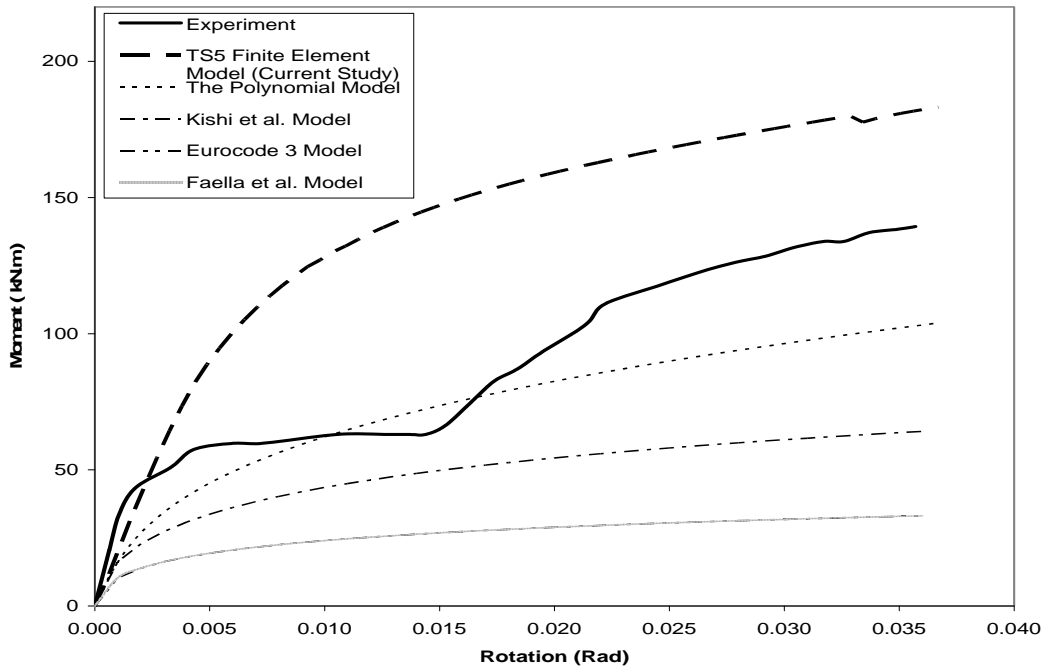


**Figure 3-12 Comparison of TS5 Specimen**



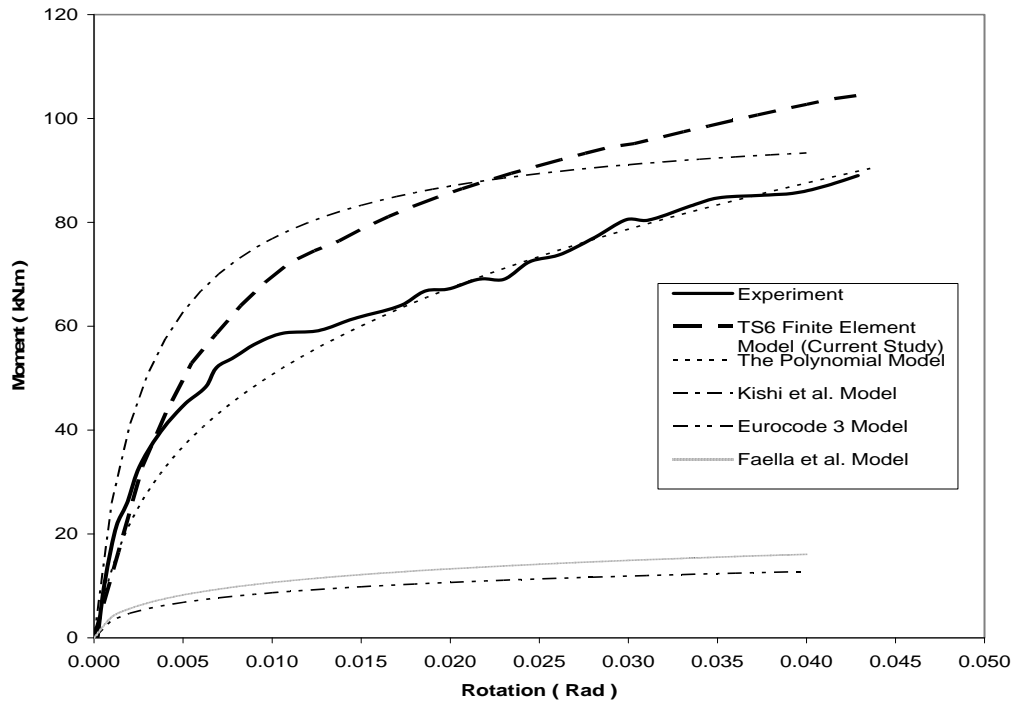


**Figure 3-13 Comparison of TS6 Specimen**

As seen from Figures 3-7 to 3-13, the polynomial model and Kishi et al. model are the best fitting ones with the experimental research, and Eurocode 3 and Faella et al. models give relatively conservative values for the moment-rotation curves. This is expected since Eurocode 3 is a code of practice which has to take the safety factors into account and must be on the conservative side. It is also observed that Faella et al. model generally produces a moment-rotation curve very close to the Eurocode 3 equation (especially the responses are identical for TS5 connection).

With regards to the comparison of the results of the current finite element study and the mathematical models, the finite element results generally produce an upper-bound solution and they are close to the polynomial and Kishi et al. models. In some analyzed connections, where the solution of the finite element model gives exaggerated results as in the case for TS5 specimen, the mathematical models are observed to produce erroneous results, as well. In this regards, both the simplified mathematical models and the 3-D finite element models can fail to replicate the physical conditions satisfactorily.

In conclusion, the comparisons done so far shows that the mathematical models can also provide accurate and reliable means for the analysis of semi-rigid connections. The current study gives an inside feeling of where the finite element models and the mathematical models that are the favorite tools of current code of practice stand.

## CHAPTER 4

### SUMMARY AND CONCLUSION

#### 4.1 Summary

The first chapter of the thesis started with an overview of the some of the failed types of connections after recent earthquakes. The connections' vulnerability points were also stated in this heading. Then a simple background history about semi-rigid connections was presented. The connection types, which are generally considered as semi-rigid, were defined and described with their properties. The general classification system for the connection types with their application ranges were defined and detailed with the help of the standard code definitions. The end of the first chapter is dedicated to the history of the finite element analyses of the semi-rigid connections and the scope of the thesis work. Previous finite element analyses conducted by various researchers were investigated, and basic definitions and details of these analyses were presented.

In the second chapter of the thesis, the difficulties that were met during the finite element analyses were listed. Selected experimental analyses for the certain semi-rigid connection types were revisited and detailed, and these are top and seat angle connections with or without double web angles. These revisited connections were converted to the finite element simulation in the concept of the thesis. The procedure of this conversion was presented with required information for the nonlinear finite element analysis. These included general configuration of the models, element types, friction coefficients, pretension values and material models. In the later part of this chapter, the comparisons of the finite element models of the thesis work with experimental analysis and the one of the other detailed finite element analyses were presented. Brief explanation for each analyzed connection

type was provided afterwards. The drawbacks of the finite element models were also discussed in this chapter. The chapter gives an inside feeling of the advantages and disadvantages of using finite element analyses for the modeling of top and seat angle connection with or without double web angles.

The third chapter of this thesis work focused on the simplified mathematical models developed by various researchers. The corresponding models definitions were reviewed and detailed with necessary formulations. The linear, multi-linear, polynomial and the power models are the models that were revisited in Chapter 3. In these models, the polynomial and power models are the more recent models. In these, the power model is divided into three categories: Kishi et al. [41] power model, Eurocode 3 [17] power model and the Faella et al. [17] power model. Then, these recent models were recalculated for the finite element simulations of the analyzed models in Chapter 2. The results of each moment-rotation curve were presented afterwards. At the end of the chapter, the comparisons of these models with finite elements simulations were briefly discussed and main body of the thesis work completed.

## **4.2 Conclusion**

The semi-rigid connection usage is very limited in today's structural engineering era. However, this type of connection is satisfactory in both economy and safety [1-3]. The remaining problems for these connections with regards to use in engineering practice are related with the structural analysis with this type of connections and the reliability of the analysis.

In this thesis, one way of analysis namely 3-D nonlinear finite element analysis of such complicated connections are performed and results are discussed. Each analysis is compared with test results and other 3-D finite element analysis where available. The differences of this thesis and the other works are emphasized. This thesis also provides an important factor in the analysis of the semi-rigid connections which is the mathematical models. The mathematical models are one of the helpful

tools when it comes to compare the analysis and test results. One of the other functions of them is the simplification of connection behavior for the purpose of use in design equations. The comparison of these simplified models in this thesis provides an insight for structural engineers to appreciate the capability of each model, where this comparison also includes one of the most referred codes (namely Eurocode 3).

The following can be listed as the main conclusions of this thesis:

- A well established three dimensional finite element simulation can predict the moment-rotation response of a semi-rigid connection within an acceptable accuracy as presented in this thesis.
- In experimental analysis, it is observed that the researchers use very strong beam sections in order to ensure the failure of a specimen connection prior to the yielding of the connecting beam (the ratio of the ultimate moment of the connection response and the plastic moment of the beam ranges from 30% to 45% in the analyzed connection types in this thesis). Furthermore, the selected column sections are provided not to go beyond elastic deformation through the selection of thick flanges and the use of stiffeners. This physical behavior is well-predicted by the presented finite element simulations in this thesis.
- The error range for the current finite element analyses can vary from zero to 45% for the initial stiffness and up to 10% for the plastic/nonlinear stiffness. Similar errors for the initial stiffness value were also observed in another finite element analysis [4].
- The ultimate moments obtained from the current finite element analyses differ from the experimental results in the order of 5% at most for the top and seat angle connection with double web angles and 25% at most for the top and seat angle connection without double web angles.

- Among the simplified mathematical models, the best fit with the experimental analyses are seen in the polynomial model. On the other hand most conservative results are obtained from Eurocode 3 models. In this respect, Eurocode 3 provides a response with a safety factor.

To conclude, the semi-rigid connections have been idealized as simple or shear connections in the literature before 1990's. This trend has been changing after reformations in code definitions. Recently, semi-rigid connections are cited more often and their performance arouses curiosity among structural engineers. By utilizing 3-D nonlinear finite element analysis, the thesis aims to show the moment-rotation performance of the some of the types of semi-rigid connections, namely the top and seat angle with or without double web angle connections. The performances of mathematical models are also tested within the thesis. Future studies related in this field might provide a successful mathematical model that will include well established theory behind with a successful experimental justification. In this viewpoint, the finite element analyses are necessary tools to guide research experts of the field towards the aimed goal. This goal will provide easier structural analysis with semi-rigid connections. Furthermore, it provides a convenient way for the analysis and retrofitting of older steel structures that were built with such connections. Consequently, it will compensate the unpopularity of semi-rigid connections and lead to more economical and safe steel structures which is the basic demand in structural engineering.

## REFERENCES

- [1] Mahin SA. "Lessons from damage to steel buildings during the Northridge earthquake." *Engineering Structures* 1998;20:261–70.
- [2] Hiroshi A. "Evaluation of fractural mode of failure in steel structures following Kobe lessons." *Journal of Constructional Steel Research* 2000;55:211–27.
- [3] Weynand K, Jaspart JP, Steenhuis M. "Economy studies of steel building frames with semi-rigid joints." *Journal of Constructional Steel Research* 1998;46:1–3
- [4] Citipitioglu AM, Haj-Ali RM, White DW. "Refined 3D finite element modeling of partially restrained connections including slip." *Journal of Constructional Steel Research* 2002;8:995–1013.
- [5] Chen W.F "Practical analysis for Semi-Rigid Frame Design" Word Scientific 2000
- [6] Krishnamurthy N, Graddy D. "Correlation between 2 and 3-dimensional finite element analysis of steel bolted end- plate connections." *Computers & Structures* 1976;6:381-389.
- [7] Krishnamurthy N. "Modeling and prediction of steel bolted connection behavior." *Computers & Structures* 1979;11:75–82.
- [8] Bursi O.S, Jaspart J.P. "Basic issues in the finite element simulation of extended end plate connections." *Computers & Structures* 1998;69:361–82.
- [9] Sherbourne A.N, Bahaari M.R. "3D Simulation of end-plate bolted connections." *Journal of Structural Engineering ASCE* 1997;120(11):3122–36.

- [10] Sherbourne A.N, Bahaari M.R. “Finite element prediction of end plate bolted connection behavior. I: Parametric Study.” *Journal of Structural Engineering ASCE* 1997;123(2):157–64.
- [11] Azizinamini A. “Cyclic characteristics of bolted semi-rigid steel beam to column connections.” PhD thesis, University of South Carolina, Columbia, 1985.
- [12] Danesh F, Pirmoz A, Saedi Daryan A. “Effect of shear force on initial stiffness of top and seat angle connections with double web angles.” *Journal of Constructional Steel Research* 2007;63(9): 1208–18.
- [13] Kukreti AR, Abolmaali A. “Moment–rotation hysteresis behavior for top and seat angle connections.” *Journal of Structural Engineering ASCE* 1999; 125(8):810–20
- [14] Yang JG, Murray TM, Plaut RH. “Three-dimensional finite element analysis of double angle connections under tension and shear.” *Journal of Constructional Steel Research* 2000;54:227–44.
- [15] Abolmaali A, Kukreti AR, Razavi H. “Hysteresis behavior of semi-rigid double web angle steel connections” *Journal of Constructional Steel Research* 2003; 59: 1057–1082
- [16] Nethercot, D.A., Zandonini, R. “Methods of Prediction of Joint Behaviour: Beam to Column Connections”, Chap. 2, in *Structural Connections: Stability and Strength*, edited by R Narayanan, Elsevier Applied Science Publisher 1990; pp. 22-62
- [17] Faella, C., Piluso, V., Rizzano, G., “*Structural Steel Semirigid Connections: Theory, Design, and Software*” CRC Press, 1999
- [18] ANSYS User Manual version 11.0 ANSYS Inc.



- [19] Astaneh-Asl, A., Nader, M. N., and Malik, L. (1989). “Cyclic behavior of double angle connections.” *Journal of Structural Engineering ASCE*, 115(5), 1101–1118.
- [20] AISC Manual of Steel Construction: Load & Resistance Factor Design 2<sup>nd</sup> Edition 1994
- [21] Specification for Structural Joints Using ASTM A325 or A490 Bolts, RESEARCH COUNCIL ON STRUCTURAL CONNECTIONS (June 30, 2004)
- [22] The AISC Specification for Structural Steel Buildings (2005)
- [23] Nelson, T., Wang, E. “Reliable FE-Modeling with ANSYS” ANSYS Web Source
- [24] McCormac, J.C., “Structural Steel Design 4<sup>th</sup> Edition” Prentice Hall 2008
- [25] Kishi N, Ahmed A, Yabuki N, Chen WF. “Nonlinear finite element analyses of top and seat-angle with double web-angle connections.” *International Journal of Structural Engineering and Mechanics* 2001;12:201–14.
- [26] Ahmed A, Kishi N, Matsuoka K, Komuro M. “Nonlinear analysis on prying of top-and seat-angle connections.” *Journal of Applied Mechanics* 2001;4:227–36.
- [27] Chan S.L, Chui P.P.T. “Non-linear static and cyclic analysis of steel frames with semi-rigid connections” 1999 Elsevier.
- [28] Lightfoot, F. and LeMessurier, A.P. (1974): “Elastic analysis of frameworks with elastic connections.” *J. Struct.Div. ASCE* 100(ST6), 1297-1309.
- [29] Romstad, K.M. and Subramanian, C.V. (1970): “Analysis of frames with partial connection rigidity.” *J. Struct. Div. ASCE* 96(ST11), 2283-2300.

- [30] Frye, M.J. and Morris, G.A. (1975): "Analysis of flexibly connected steel frames." Canadian Journal of Civil Engineering. 2(3), 280-291.
- [31] Sommer, W.H. "Behaviour of Welded Header Plate Connections", MS Thesis University of Toronto, ON, Canada 1969
- [32] Picard, A., Giroux, Y.M and Burn, P. (1976) Discussion of "Analysis of flexibly connected steel frames." by Frye, M.J. and Morris, G.A., Canadian Journal of Civil Engineering., 3, 2, 350-352.
- [33] Altman, W.G. Jr., Azizinamini, A., Bradburn, J.H., and Radziminski, J.B. "Moment-rotation characteristics of semi-rigid steel beam to column connection", Dept. of Civ. Engrg., Univ. of South Carolina, Columbia, S.C., 1982
- [34] Batho, C. and Rowan, H.C. "Investigation on Beam and Stanchion Connections", 2nd Report, Steel Structures Research Committee, Dept. of Scientific and Industrial Research, His Majesty's Stationary Office, London, 1934 Vols. 1-2, pp. 61-137.
- [35] Krishnamurthy, N., Huang, H.T., Jeffrey, P.K. and Avery, L.K. (1979): "Analytical M- $\theta$  curves for end-plate connections." J. Struct. Div. ASCE 105(ST1), 133-145.
- [36] Colson, A. and Louveau, J.M., "Connections Incidence on the Inelastic Behavior of Steel Structural", Euromech Colloquium 174, 1983
- [37] Richard, R.M. "A Study of Structural Systems Having Conservative Nonlinearity", Ph.D. Thesis, Purdue Univ., West Lafayette, IN 1961
- [38] Goldberg, J.E. and Richard, R.M. (1963): "Analysis of nonlinear structures." J. Struct. Div. ASCE 89(ST4).

[39] Attiogbe, E., and Morris, G. (1991). "Moment-rotation functions for steel connections" *Journal of Structural Engineering*, ASCE, 117(6), 1703–1718

[40] Kishi N, Chen WF. "Moment-rotation relations of semi-rigid connections with angles." *Journal of Structural Engineering*, ASCE 1990;116(7):1813–34

[41] Kishi N, Chen WF. Hasan, R., and Matsuoka, K. G., (1993) "Design aid of semi-rigid connections for frame analysis," *Engineering Journal*, AISC, 3<sup>rd</sup> Quarter, pp. 90-107

[42] CEN (1997) Eurocode 3, 1.1 Joint in Building Frames (Annex J), Approved Draft, January, CEN/TC250/SC3-PT9, Comité Européen de Normalisation